MEASUREMENT OF INSTANTANEOUS VELOCITIES FROM A FLUIDICALLY CONTROLLED NOZZLE USING A LASER DOPPLER VELOCIMETER

Michael Kenneth Hollis

DUDLEY KNOX LIBRARY,
NAVAL POSTGRADUATE SCHOOL
MONTEREY, CALIF. 93940

NAVAL POSTGRADUATE SCHOOL
Monterey, California

THESIS

MEASUREMENT OF INSTANTANEOUS VELOCITIES
FROM A FLUIDICALLY CONTROLLED NOZZLE
USING A LASER DOPPLER VELOCIMETER

by

Michael Kenneth Hollis

September 1976

Thesis Advisor: D. J. Collins

Approved for public release; distribution unlimited.

T175005

SECURITY CLASSIFICATION OF THIS PAGE (When Data Entered)

REPORT DOCUMENTATION PAGE		READ INSTRUCTIONS BEFORE COMPLETING FORM
1. REPORT NUMBER	2. GOVT ACCESSION NO.	3. RECIPIENT'S CATALOG NUMBER
4. TITLE (and Subtitle) Measurement of Instantaneous Velocities From a Fluidically Controlled Nozzle Using a Laser Doppler Velocimeter		5. TYPE OF REPORT & PERIOD COVERED Master's Thesis September 1976 6. PERFORMING ORG. REPORT NUMBER
7. AUTHOR(s) Michael Kenneth Hollis		8. CONTRACT OR GRANT NUMBER(s)
9. PERFORMING ORGANIZATION NAME AND ADDRESS Naval Postgraduate School Monterey, California 93940		10. PROGRAM ELEMENT, PROJECT, TASK AREA & WORK UNIT NUMBERS
11. CONTROLLING OFFICE NAME AND ADDRESS Naval Postgraduate School Monterey, California 93940		12. REPORT DATE September 1976 13. NUMBER OF PAGES 87
14. MONITORING AGENCY NAME & ADDRESS(if different from Controlling Office) Naval Postgraduate School Monterey, California 93940		15. SECURITY CLASS. (of this report) Unclassified 15a. DECLASSIFICATION/DOWNGRADING SCHEDULE

16. DISTRIBUTION STATEMENT (of this Report)

Approved for public release; distribution unlimited.

17. DISTRIBUTION STATEMENT (of the abstract entered in Block 20, if different from Report)

18. SUPPLEMENTARY NOTES

19. KEY WORDS (Continue on reverse side if necessary and identify by block number)

20. ABSTRACT (Continue on reverse side if necessary and identify by block number)

A laser Doppler velocimeter was used to investigate the flow field produced by an oscillating jet. Velocity measurements were made with the fluidically controlled jet in both the oscillatory and non-oscillatory modes. Mean and instantaneous surveys were made to quantify the time dependent nature of the jet.

DD FORM 1 JAN 73 1473 EDITION OF 1 NOV 65 IS OBSOLETE
S/N 0102-014-6601 |
(Page 1)

SECURITY CLASSIFICATION OF THIS PAGE (When Data Entered)

Measurement of Instantaneous Velocities From a Fluidically Controlled Nozzle Using A Laser Doppler Velocimeter

by

Michael Kenneth Hollis
Lieutenant, United States Navy
B.S., United States Naval Academy, 1969

Submitted in partial fulfillment of the
requirements for the degree of

MASTER OF SCIENCE IN AERONAUTICAL ENGINEERING

from the

NAVAL POSTGRADUATE SCHOOL
September 1976

DUDLEY KNOX LIBRARY,
NAVAL POSTGRADUATE SCHOOL
MONTEREY, CALIF. 93940

ABSTRACT

A laser Doppler velocimeter was used to investigate the flow field produced by an oscillating jet. Velocity measurements were made with the fluidically controlled jet in both the oscillatory and non-oscillatory modes. Mean and instantaneous surveys were made to quantify the time dependent nature of the jet.

TABLE OF CONTENTS

I. INTRODUCTION ---------- 6

A. OBJECTIVES ---------- 6

B. EXPERIMENTAL APPROACH ---------- 7

II. LASER DOPPLER VELOCIMETRY ---------- 11

A. DOPPLER PRINCIPLE ---------- 11

B. OPTICAL MODES OF OPERATION ---------- 12

1. Reference Beam Mode ---------- 13

2. Dual Scatter Mode ---------- 14

3. Single Beam Mode ---------- 15

C. CHOICE OF OPTICAL ARRANGEMENTS ---------- 16

D. SIGNAL PROCESSORS ---------- 17

III. OSCILLATING FREE JET ---------- 20

IV. EXPERIMENTAL SETUP ---------- 23

A. GENERAL ---------- 23

B. APPARATUS ---------- 24

C. JET AND TRAVERSING MECHANISM ---------- 25

D. LDV SUPPORT ASSEMBLY ---------- 26

E. LDV COMPONENTS ---------- 27

F. PARTICLE GENERATOR ---------- 29

G. PULSE GENERATOR ---------- 30

V. OPERATIONAL CONSIDERATIONS FOR THE LDV ------- 32

A. GENERAL ---------- 32

B. COUNTER PROCESSOR OPERATION ---------- 32

C. BAND-PASSING ---------- 37

VI. EXPERIMENTAL PROCEDURE ---------- 41

A. ALIGNMENT OF OPTICS ---------- 41

B. MEASUREMENTS OF THE NON-OSCILLATING JET FLOW ---------- 43

C. MEASUREMENTS OF THE OSCILLATING JET FLOW ---------- 47

VII. EXPERIMENTAL RESULTS ---------- 50

A. MEAN VELOCITY MEASUREMENTS OF NON-OSCILLATING JET ---------- 50

B. TURBULENCE INTENSITY MEASUREMENTS -------- 51

C. MEAN VELOCITY MEASUREMENTS OF OSCILLATING JET ---------- 51

D. INSTANTANEOUS VELOCITY MEASUREMENTS OF OSCILLATING JET ---------- 52

VIII. CONCLUSIONS ---------- 55

LIST OF REFERENCES ---------- 86

INITIAL DISTRIBUTION LIST ---------- 87

I. INTRODUCTION

A. OBJECTIVES

The overall objective pursued in the course of this thesis was to gain additional knowledge which could be applied to the study of thrust augmentation. Thrust augmentation has become an increasingly important area of research in the last few years as the need for high performance vertical short take-off and landing (V/STOL) aircraft has been recognized.

It has been found that significant thrust augmentation is possible through the use of oscillating jets. Such jets, by flipping from side to side, are able to generate increased thrust by entraining a relatively large secondary flow.

An oscillating jet was chosen as the subject of this thesis as it is an interesting and not fully understood means of thrust augmentation. The jet under investigation was a fluidic device in that it was made to oscillate by means of a fluidic feedback loop. Due to the diverse applications of fluidic devices (thrust augmentation, fuel injectors, logic circuits, etc.) it was felt that a

significant contribution could be made by further study of the associated flow phenomena.

Velocity measurements of the jet's flow field were made with a laser Doppler velocimeter (LDV). The LDV is a relatively new means of determining flow velocities which is being applied to a number of difficult measurement situations, such as between blade rows in turbomachinery. A secondary objective, therefore, was to gain familiarity with the LDV and its possible applications.

The LDV was chosen primarily, however, because of its ability to make measurements not possible with more conventional apparatus, such as pitot tubes, and to do so without the use of flow disturbing probes and wires. The ability of the LDV to sample instantaneous velocities with the flow in a given part of the oscillatory cycle made its application to the jet study particularly appropriate.

B. EXPERIMENTAL APPROACH

The first stage of the experiment involved measurements of the jet in the non-oscillatory mode. With the feedback loops disconnected the jet remained stationary, producing a classic near-Gaussian velocity profile. This permitted a comparison with theoretical results [10] to ensure that the LDV was operating properly.

As flow characteristics at that point were well known, time was available for refining the experimental setup to deal with vibrational limitations, particle generation and seeding of the flow. These problems were solved before examining more complicated flow situations in order to avoid the possibility of gathering false data due to flaws in the basic experimental arrangement.

An additional advantage to working with a stationary jet was that LDV measurements could be roughly verified by means of pitot tube surveys. Although exact agreement was neither expected nor obtained, the comparison served to provide a baseline confidence for the electronic setup. Additionally, preventing the oscillations allowed measurements of the jet's turbulence factor to be made.

The second phase of the experimentation involved measurements of the jet in the oscillating mode. Mean velocity surveys like those done for the stationary jet were made first. Simultaneous measurements with the LDV and pitot tubes were done once again for comparison purposes.

The final step was measuring the instantaneous velocity profile of the oscillating jet. This required measuring velocities in a plane at a given distance from the jet exit while the jet was at a desired orientation in its

oscillating cycle. This approach is shown schematically in Figure 1. By mounting a pressure transducer at the exit it was known when the jet was on the transducer's side of the exit, since that produced the peak signal from the pressure transducer. Thus, instantaneous velocities could be measured throughout the field, if data samples were taken only at times of peak pressure, or at known times after peak pressure.

This "strobing" of the flow was accomplished by using a pulse generator to activate or inhibit the counter module at the desired times. As shown in Figure 2, the peak pressure signal was used as an external trigger for the pulse generator. After a selectible delay period, a pulse was generated which activated the counter (permitting velocity measurement to be made) for the duration of the pulse. Conveniently, the counter was transistor to transistor logic (TTL) compatible, so a pulse constituted a logical "1", or high state, which activated the counter. Similarly, the absence of a pulse constituted a logical "0", inhibiting the counter.

Measurements could, theoretically, be made with the jet in any orientation by merely selecting the proper delay time. The jet continues to move during the measurement,

of course, but this effect could be made negligibly small by choosing a pulse width that was only a small percentage of the total cycle.

In the following sections background information on the LDV has been provided so that the reader who is unfamiliar with laser Doppler velocimetry (or anemometry as it is often called) might better understand its application to the study of the fluidically controlled jet.

II. LASER DOPPLER VELOCIMETRY

A. DOPPLER PRINCIPLE

The laser Doppler velocimeter is a device which provides direct measurement of flow velocities. The basic principle is as follows. [1] Laser light is focused into a flow which contains small particles (naturally present or artificially seeded) capable of scattering the light (Figure 3). Consistent with the Doppler principle, the scattered light undergoes a frequency shift according to equation (1):

$$f_s = f_i + \frac{1}{L} \bar{v} \cdot (\hat{e}_s - \hat{e}_i) \qquad (1)$$

where

f_s = frequency of scattered light

f_i = frequency of incident light

$\hat{e}_s$ = unit vector in scattering direction

$\hat{e}_i$ = unit vector in incident direction

$\bar{v}$ = velocity vector

L = wavelength of incident light

The frequency shift is seen to be:

$$f_d = f_s - f_i \qquad (2)$$

The equation for the Doppler frequency, f_d, therefore, is:

$$f_d = \frac{1}{L} \bar{v} (\hat{e}_s - \hat{e}_i) \qquad (3)$$

Equation (3) shows a particularly significant result: the relationship between the light frequency shift and the instantaneous velocity is a linear one. For this reason, a LDV is more suited for making velocity measurements in highly turbulent regions, than is the hot wire anemometer, for example, since nonlinear characteristics are not present. [2]

The Doppler frequency shift is measured by heterodyning the light scattered by the particles with unscattered light from the same laser. The heterodyning is performed optically on the surface of a photomultiplier (PM) tube. [3] The output of the PM tube is processed by one of several methods (discussed subsequently) and the flow velocity is displayed.

B. OPTICAL MODES OF OPERATION

There are three basic arrangements of the illuminating optic (laser and components needed to focus beam into the flow) and the collecting optic (lenses, diaphrams, and photomultiplier):

-Reference-beam mode (local oscillator heterodyning)

-Fringe mode (dual scatter)

-Single beam mode

1. Reference-Beam Mode

The reference-beam mode, first used by Yeh & Cummings (1964), is shown in Figure 4.a. Two beams of different in-intensities are focused at a point in the flow. The reference beam is the weaker of the two, as it is filtered before passing through the flow. It is the brighter "reference" for the photomultiplier tube, however, as it is aligned to pass directly into the tube after penetrating the flow. Thus the photodetector sees a mixture of direct light from the reference beam and the Doppler shifted light of the second beam which is scattered by particles in the flow.

This configuration, shown vectorially in Figure 4.b., may be described more completely by applying equation (1) to beam 2 (the scattered beam), yielding,

$$f_2 = f_i + \frac{\overline{V}}{L} \cdot (\hat{e}_s - \hat{e}_i)$$

The reference beam is unscattered and therefore undergoes no frequency shift. As a result, the photo-detector will have an output current composed of a DC term from the reference beam and an AC term from beam 2 which varies with f_d as follows: [4]

$$f_d = f_2 - f_i = \frac{\overline{V}}{L} \cdot (\hat{e}_s - \hat{e}_{i2})$$

2. Dual Scatter Mode

The fringe or dual scatter mode shown in Figure 5.a. was first proposed by Rudd (1969). In this arrangement two beams of equal intensity are crossed in the flow to produce a real fringe pattern. As seen in Figure 2.b., the two incident beams result in two scattered beams according to equation (1):

$$f_{s1} = f_i + \frac{\overline{V}}{L} \cdot (\hat{e}_s - \hat{e}_{i1})$$

$$f_{s2} = f_i + \frac{\overline{V}}{L} \cdot (\hat{e}_s - \hat{e}_{i2})$$

Combining the beams yields the Doppler frequency:

$$f_d = f_{s2} - f_{s1} = \frac{\overline{V}}{L} \cdot (\hat{e}_{i1} - \hat{e}_{i2})$$

The absence of e_s in this equation shows that the detected frequency is no longer dependent on the scattering direction. This permits the use of a lens to collect scattered light in a wide angle, providing greater intensities for the photodetector.

A second means of describing the phenomena involved in the dual scatter arrangement is based on the fringe pattern formed by the intersecting beams. This approach

provides a relatively simple model which is helpful in explaining the operation of the counter processors discussed in later sections.

Since the two crossing beams are coherent and of equal intensities, a set of closely spaced interference fringes form in the "focal volume" where the intersection takes place. As seen in Figure 5.c., dark bands result where the light beams add destructively (destructive interference) and light bands result where they add constructively (constructive interference).

When particles in the flow traverse this "picket fence" of alternatingly light and dark bands, they scatter light only while in the light bands, generating a current at the photodetector. The current fluctuation will be proportional to the frequency at which particles cross the fringes, i.e., proportional to the velocity component of the particles that is parallel to the plane defined by the two intersecting beams.

3. Single Beam Mode

The single beam mode, also known as "virtual fringe" [4] and "interferential Doppler" [2] is shown in Figure 6.a. A single laser beam is directed into the flow, scattering with different intensities in all directions.

Light scattered in two chosen directions is collected symmetrically about the system axis. For the two directions, the frequencies are:

$$f_{s1} = f_i + \frac{\overline{V}}{L}\cdot(\hat{e}_{s1}-\hat{e}_i)$$

$$f_{s2} = f_i + \frac{\overline{V}}{L}\cdot(\hat{e}_{s2}-\hat{e}_i)$$

Combining the two optically (lens and mirror arrangement in Figure 6.a.), yields:

$$f_d = \frac{\overline{V}}{L}\cdot(\hat{e}_{s2}-\hat{e}_{s1})$$

This result is almost the same as for the dual scatter mode. The symmetry of the equations is also applicable to the fringe interpretation of the phenomena. The difference, however, is that in this case the fringes are virtual instead of real.

C. CHOICE OF OPTICAL ARRANGEMENTS

Choice of which of the three fundamental operating modes to apply is dependent upon the flow situation encountered. Dual scatter and single beam modes are well suited to flows with low density of scatter (like gas-particle flows). [4] Reference-beam mode, on the other hand behaves well with high concentrations.

One important advantage of the dual scatter and single beam modes is that they allow for collection of light on the same side as the illuminating optic. This back-scattering is useful when it is difficult to set up instrumentation on two sides of a flow field.

In general, with gas particle flows, the dual scatter system is the easiest to set up. [4] If two velocity components are desired simultaneously, however, the single beam mode is best. This is because it is relatively simple to add an additional photomultiplier tube and set of mirrors to collect light scattered in another direction (i.e., another velocity component).

D. SIGNAL PROCESSORS

Thus far the basic arrangements of the illuminating and collecting optics have been described. For each of these there are three means of processing the signal from the LDV photodetector:

- spectrum analyzers
- frequency trackers
- counters

The spectrum analyzer is useful in situations where only a mean velocity is desired. The analyzer measures the frequency spectrum of the Doppler signal itself. The

peak in the spectrum corresponds to the mean velocity, and the width of the peak is related to the turbulence intensity. As frequency measurements are generally limited to approximately 100 KHz, the analyzers are limited to low velocity (less than one meter/second) flows.

Frequency trackers convert Doppler frequency to an analog voltage which is proportional to the instantaneous velocity. If the tracker is provided with a continuous signal (no drop out), it provides a continuous output similar to that obtained from hot wires. Although drop out control devices can be used to provide a dummy signal to the tracker when no LDV signal is present (due to low concentration of scattering particles), a point is reached at which the validity of the result is in doubt. Trackers are best applied in situations of high concentration of scatter and a low percentage of drop out. [4]

Counter systems are, in principle, the most simple processors. Each time a signal is received from the photodetector, indicating fringe crossing by a particle, a "count" accumulates in a counting register. Knowing the distance traveled by the particle (the number of "counts" times the fringe spacing) and the time elapsed (generally measured by a 250 MHz clock) the velocity is easily computed.

There are several complications which can arise, such as bad signals from particles crossing the edge of the focal volume. As a counter processer was used in this thesis, the actual operation and limitations are discussed in a later section.

III. OSCILLATING FREE JET

The flow examined in this thesis was produced by a free jet which was made to oscillate by fluidic means. This jet is typical of a number of devices which are the products of fluidics technology.

Many types of devices have been developed and used in a wide variety of applications. [5] Many are used in fluidic logic circuits to perform logic functions (such as OR, AND, NOR, etc.). Jets such as the one studied in this thesis have been employed successfully in these circuits.

Depending on the type of device used, there are various means of controlling the output characteristics. One means, used in the turbulence amplifier (a jet), is to control the jet's Reynolds number, and hence the laminar to turbulent transition.

The free jet used in this thesis, however, was controlled by means of small pressure signals applied to the flow. Viets' paper on fuel injectors presents an explanation of the manner in which the pressure signals cause the jet to oscillate. [8]

As seen in Figure 7, compressed air flows through a contraction section into an expansion section. At the

throat (0.635 x 5.08 cm) were located two control ports for attachment of the feedback loop. With the ports sealed (Figure 7.a.) the jet acted as a conventional free jet with a rectangular exit cross section (1.03 x 5.08 cm). With the ports open and connected by the feedback loop (Figure 7.b.), the jet became bistable in nature, alternatingly attaching to wall A and then to wall B.

The bistable or flipping nature of the jet is due to pressure fluctuations at the control ports. The fluctuations occur as pressure waves propagate through the feedback loop. A compression wave travels in one direction, say A to B, as an expansion wave travels from B to A. The compression wave is created by the jet attaching itself to wall A, and the expansion wave is created by the jet detaching from wall B. The attachment/detachment sequence results in an oscillation of the jet, since the jet always returns to the low pressure wall (which becomes the high pressure wall when the jet arrives).

For an ideally designed and constructed device, the jet continually flips from one side to the other with no appreciable residence time on either wall. This is not necessarily the case, however. Due to slight imperfections in the construction of the nozzle (which effectively changes

the symmetry of the design) the jet will, in general, show a natural preference to attach to a particular wall for a significant portion of its period. Even so, oscillatory frequencies on the order of 100 Hz at a stagnation pressure of 5 psig can be expected. [8]

Viets determined that, as is expected intuitively, increasing the length of the acoustic feedback loop decreases the oscillatory frequency (longer distance for the waves to travel), and that increasing the stagnation pressure increases the frequency.

IV. EXPERIMENTAL SETUP

A. GENERAL

Choice of suitable locations for conducting the experiments was constrained by two requirements: compressed air source for the jet, and ventilation necessitated by the seeding particles exhausted from the jet. The 5'x5' smoke tunnel at the Naval Postgraduate School was used in all but the most preliminary experiments, as it filled the above requirements and offered other advantages as well.

The tunnel, conveniently located in the basement of Halligan Hall, was equipped with a small control room from which the tunnel test section could be observed. This proved particularly useful, as the jet was placed in the test section, while the necessary electronic equipment and research personnel remained in the control room, free from the effects of the seeding particles.

A plexiglass wall separating the test section and control room was effective in keeping the seeding particles out of the control room, in spite of the existence of a hole to permit the laser/transducer assembly to extend into the tunnel. The wall was not particularly effective,

however, in attenuating the loud jet noise so ear protectors were worn during extended sessions.

Figure 8 shows the smoke tunnel-control room orientation in the basement. As can be seen in the photograph, considerable clearance existed beneath the tunnel test section. This area was chosen for positioning the seeding particle generating apparatus.

B. APPARATUS

The following apparatus, located in the vicinity of the smoke tunnel as described above, constituted the major articles necessary to conduct the thesis:

1. Rectangular exit area (1.03 x 5.08 cm) jet, of plexiglass construction, with an aluminum reservoir and tubular feedback loop.
2. LDV components:
   - Laser
   - Transducer
   - Photomultiplier tube
   - Display module
3. Pressure transducer and associated power supply.
4. Amplifier to condition transducer signal for input to counter.
5. Pitot tube and water filled U-tube.

6. Support assembly for LDV optical components.
7. Oscilloscope
8. Traversing mechanism (structure, motor, and control box) for moving the jet vertically.
9. Oil burning particle generators (5) with heat control rheostats, and feed lines to jet reservoir.
10. Pulse generator

In the following sections the above apparatus will be discussed in greater detail.

C. JET AND TRAVERSING MECHANISM

Figure 9 shows a schematic of the jet and some pertinent dimensions. As can be seen, the feedback loops are connected to aluminum fittings extending from the plexiglass housing. The loops were removed for a portion of the experiments and the fittings were sealed with modeling clay. A better view of the jet and fittings is available from the photograph in Figure 10.

In order to accomplish velocity surveys of the jet's flow field, it was necessary to move either the jet or the optics in a vertical direction. As the optical components are very sensitive to motion (vibration) and alignment, it was decided to keep them stationary and traverse the jet

instead. Figure 11 shows the device which positioned the jet.

As can be seen, the jet reservoir was attached to a plate which moved vertically on two threaded rods when the electric motor was activated. A pointer was attached to the reservoir to indicate the position of the jet centerline relative to the scale on the immobile portion of the traversing mechanism. The "zero" of the scale was aligned so that a zero reading indicated that the laser beam intersected the jet centerline. All scale readings, therefore, indicated the distance between the centerline and the point at which velocity was being measured (the laser beam).

D. LDV SUPPORT ASSEMBLY

Operation of an LDV system is dependent on a low vibration level environment. If vibrations are excessive, fringe patterns are lost and measurements are impossible. For this reason, the laser, transducer and photomultiplier tube were isolated from the vibrations of their surroundings. Large aluminum posts were secured to the concrete basement floor by bolts shot into the concrete. Cut-ways were made into the control room floor and the side of the tunnel (see Figure 12) so that the beams were touching only the basement floor. The optical components were mounted on the

beams, and as such were virtually immune to vibrations. Some vibrations were transmitted by the floor itself when the air compressors were in operation, but they posed no problem.

E. LDV COMPONENTS

The LDV system was composed of a 15 milliwatt Spectra-Physics helium-neon gas laser in conjunction with the DISA 55L laser Doppler anemometer Mark II. The latter consists of the 55L90 LDA counter processor, the 55L88 LDA transducer and the 55L12 photomultiplier. The counter processor is a single unit housing five modules that process the signals from the photomultiplier.

The counter processor modules are as follows:

55L92 data rate module

55L93 digital to analog converter module

55L94 mean velocity computer module

55L95 counter module

55L97 high voltage supply module

The functions of each of the components used in the experiments will be described briefly to show the system capability.

The transducer is an integrated optoelectronic unit which was operated in the forward scatter, single channel

mode. The transducer splits the incoming laser beam and provides selection of three beam separations (80, 40, 20mm) and three focal lengths (120, 300, 600mm). The beam separation (distance between light beams leaving the transducer) determines the angle between the beams for a given focal length. The focal length is the distance from the transducer to the point at which the beams cross, i.e. the focal volume. The experimental configuration was with 80mm beam separation and a 300mm focal length. The 300mm length placed the transducer and photomultiplier tube inside the smoke tunnel, but outside the region of influence of the jet.

The photomultiplier tube was positioned approximately 308mm from the focal volume. Meniscus lenses which should have provided the PM tube with 120, 300, and 600mm focal lengths were provided, but actual lengths were found to vary somewhat. For the nominal 300mm lens, a distance of 308mm from the beam crossing provided optimum focus and signal strength.

The 55L92 data rate module provided a data rate per cent validated digital display. The role of this module is explained in detail in a later section dealing with the counter operating principles.

The mean velocity computer module gives a digital display of the mean flow velocity or the Doppler frequency. The velocity computation is based on the number of validated samples (ensemble width), and the comparator accuracy selected. This is described more completely in the counter section.

The high voltage supply module indicates voltage applied to the PM tube and current output by the PM tube. The latter information is valuable as it is an indication of how well the tube is focused on the focal volume, as well as particle concentration.

The 55L95 counter module provides a means for selecting proper bandpassing for the Doppler frequency, setting trigger levels for rejection of large particle data, and attenuation of the preamplified PM tube signal. Specific details are given in the operating procedures section.

Figure 13 shows the face of the front face of the 55L90 counter processor. The component modules are easily distinguished by the vertical divisions on the face.

F. PARTICLE GENERATOR

Particle generation was accomplished by using a gang of five bottles of oil, each containing a heating filament and

exhausting smoke into a common line. Initially the bottles were pressurized, and the smoke was routed directly to the jet's reservoir by a feed line. Problems with sealing the smoke bottles and overheating of tubing prompted the abandonment of the pressurization approach. The above problems were eliminated by attaching the common feed line for the bottles to the compressed air line that powered the jet. A venturi type connection of the two lines was used so that the smoke was sucked from the bottles, allowing them to be vented to the atmosphere without "leaks."

Although five bottles were available for operation, it was only necessary to use two at a time. This allowed rotation among the bottles, so that there was no danger of excessive heating of tubing and bottles.

Figure 14 shows a photograph of the bottle arrangement and connection to the compressed air line. Not visible in the picture are the temperature control rheostats located in the control room.

G. PULSE GENERATOR

The pulse generator was an integral part of the instantaneous velocity measurements. A Monsanto 500A generator was used as it provided the capability of controlling the

delay time (time between trigger input and pulse generation) and pulse width. Additionally, an external trigger capability was available so that interfacing between the pulse generator and pressure transducer was possible. Adjustment of the trigger level permitted triggering only off of the strongest portion of the signal (which corresponded to the jet being attached to the exit wall).

The output of the pulse generator was fed into the AUX terminal of the counter module, thus inhibiting or activating the counter. The AUX terminal had to be connected to the proper pins, as the counter is normally in an activated only status.

V. OPERATIONAL CONSIDERATIONS FOR THE LDV

A. GENERAL

The basic information necessary to use the 55L90 LDA counter processor is given in the appropriate instruction manual, Reference 8. The manual presents a combination of background information on operating principles as well as procedure to be followed in actual operation of the equipment.

As the operating principle of the counter is fundamental in understanding the manner in which an LDV system is able to present velocity information, it is discussed in detail in the following sections. The above manual is the basic reference since the descriptions are tailored specifically to the DISA equipment.

B. COMPUTER PROCESSOR OPERATION

As pointed out in an earlier section, the basic idea of the counter is that velocity can be computed by knowing the time taken for a particle to travel a known distance. The known distance is the fringe spacing, which is input to the counter module in the form of a scale factor (actually dialed in by means of thumbwheels). The PM tube

detects the passage of the known distances, since a particle reflects light each time it passes through a bright fringe in the focal volume formed by the intersecting laser beams.

Although velocity could be computed based on the time taken for a particle to traverse a single fringe, this is not done in practice. In essence, what takes place is that the times to travel across a small number of fringes (typically 5 or 10) and a larger number of fringes (8 or 16) are registered. A comparison of the time to cross the smaller number of fringes is then made with the appropriate fraction (5/8 or 10/16) of the time to cross the larger number. If the two times are equal (within some predetermined tolerance), then a "valid" measurement is said to have taken place, and the velocity data are output. This is a highly simplified explanation, but illustrates the underlying logic.

The process is seen in more detail by referring to Figure 19. Since the fringes at the edges of the focal volume are of weaker intensity than those at the center, a trigger level of 200 mV is used to set a threshold for usable indication of a fringe crossing. Each fringe crossing that has amplitude greater than 200 mV results in the creation of a logical "1" by the Schmitt Trigger-2.

As Figure 14 indicates, the logical "1"s (the fringe crossings) are counted in a fringe counter. The fringe counter activates a high count register and a low count register. The low count register accumulates C_L 250 MHz clock counts during the time it takes for N_L fringe crossings to occur. As indicated previously, N_L is typically 5 or 10 (5 will be assumed for the remainder of the explanation). Similarly, the high count register accumulates C_H clock counts until N_H fringes have been crossed (N_H of 8 will be assumed). N_L and N_H may be selected as 5 and 8, or 10 and 16 as is desired, but C_L and C_H obviously will depend on the time required to cross the N_L, N_H fringes.

After 5 fringe counts have been registered at the fringe counter, the low count gate is closed and no further clock counts are accepted by that register. After a total of 8 fringe counts have occurred, the high count gate is also closed. At this point the comparator performs the following test:

$$100 \quad \frac{C_H - \frac{8}{5} C_L}{C_H} \leq \text{epsilon ?}$$

where epsilon is the COMPARATOR ACCURACY selected on the 55L95 counter module. Values of 1.5, 3, 6, and 12 per cent are available.

The comparison is necessary to avoid false data inputs. If a fringe count is initiated at the end of a Doppler burse, i.e., by a particle crossing the last "usable" fringe in the focal volume or entering the focal volume at a steep angle to the fringes (slant entry), it will not be completed until some time during the next burst. This could permit a large number of clock counts to accumulate in the low count register (and would result in an erroneous velocity if time to travel, say 5 fringes, was the basis of calculations). The false data will be thrown out, however, since the comparator test will not be passed.

An indication of the number of samples that are able to pass the comparator's test is provided by the 55L92 data rate module. The module indicates % VALIDATED, that is how many hundreds of the last thousand samples passed the test. Validation rates under 500 with a comparator accuracy of 1.5 selected, indicate improper seeding conditions or poor alignment of the optics.

Once validation takes place, the raw velocity data at the counter module output is passed to the 55L94 mean velocity computer. The computer has a provision for selecting either 1, 16, 256, or 4096 validated velocity calculations to be used in evaluating the mean velocity

which is displayed digitally. These numbers, known as the ensemble widths, permit the operator to determine the extent of averaging desired in a given data run. If turbulence factors are to be determined, for instance, an ensemble width of 1 would be chosen, as this would most closely represent an instantaneous velocity. A larger width, on the other hand, would be appropriate for mean velocity surveys.

Another control available to the operator is the ability to select the THRESHOLD WINDOW on the counter module. This is a setting, shown in Figure 15, that determines the maximum allowable amplitude in a Doppler burst. Bursts that are much larger in amplitude than the norm for a given data run may be assumed to be from large particles. Amplitudes exceeding the threshold setting are not used, since the large particles which produced them may not be tracking the flow adequately. The burst amplitude is controlled by a combination of PM tube aperture, high voltage supply and amplifier gain. Once these parameters are set, the THRESHOLD WINDOW is adjusted to yield the highest validation rates attainable.

C. BANDPASSING

The signal coming from the PM tube to the counter is first sent to a 25 dB preamplifier and then passed to an attenuator (Figure 17). The attenuator can be varied between 0 and -31 dB by means of the AMPLIFIER GAIN buttons on the counter module. The effect of changes in the gain may be clearly seen by the changes in amplitude of the Doppler bursts when viewed on an oscilloscope.

As seen in Figure 17, the signal is next amplified by 35 dB and bandpass filtered at the filter board. The bandpassing is done to remove high and low frequency noise, i.e., to chop off the Doppler pedestal.

Bandpassing is accomplished by selection of HIGH PASS and LOW PASS values on the counter module. The LOW PASS selector removes high frequency noise, that is, it passes frequencies lower than what is selected. Similarly, the HIGH PASS removes the low frequency noise, passing frequencies higher than what is selected.

LOW PASS selections available are .256, 1, 4, 16 and 100 MHz. HIGH PASS selections are 1, 4, 16, 64, 256 KHz and 1, 4, 16 MHz. As Figure 18 illustrates, the LOW and HIGH PASS bands overlap to some extent. The extent to which the overlapping occurs is extremely important in the selection of band widths.

It is desirable to achieve the narrowest possible bandpassing of the actual Doppler frequency. If the Doppler frequency were 18 MHz, for example, the proper bandpass would be LP = 100 MHz and HP = 16 MHz. This would elminate the undesirable noise to the maximum extent practicable. The danger, of course, is bandpassing too tightly and actually eliminating the proper frequency.

If the actual frequency is 3 MHz and the high pass filter is set at 4 MHz or the low pass filter is set at 1 MHz, then the signal will be eliminated altogether. When measuring steady flows this is easily recognized when it occurs, as the velocity display will not update and the oscilloscope will indicate a very small signal. The problem is more acute when measuring turbulent flows, since a velocity distribution is involved and the bandpass might center on a minor secondary velocity of statistically little importance.

A DIGITAL HIGH PASS X2 option is available to allow tighter bandpassing. With this in effect, selecting a HP setting of say 4 MHz results in an actual HP setting of twice that selected, or 8 MHz. Care must be exercised in using this option, as use of very tight bandpass will result in reading the frequency of the center of the band

rather than the actual Doppler frequency. This phenomenon was observed when velocity measurements on the order of a few meters per second were made.

The Doppler frequency being used may be read directly from the mean velocity computer module if the proper scale factor is input. The relationship between the velocity magnitude and the Doppler frequency is given by:

$$v = cf_d$$

where

$$c = \frac{L}{2} \sin \frac{\theta}{2}$$

and

θ = beam intersection angle

The scale factor is equal to 075, or 173 for the experiments conducted. Thus with 173 in the scale factor window, the digital output will be velocity in meters per second. With 075 in the window, the output will be f_d, the Doppler frequency, in MHz.

Knowing the value of c permits one to calculate an approximate value of f_d if an approximate flow velocity is known. This is useful as it provides a basis for initial bandpass selection. If the approximate velocity is substantially in error, this will be apparent from the oscilloscope display and corrections can be made.

Bandpassing is one of the most critical parameters available to the operator and should be adjusted and tested continuously as different flow regions are measured.

VI. EXPERIMENTAL PROCEDURE

A. ALIGNMENT OF OPTICS

The first step in any data taking sequence was to insure that the optical components were aligned properly. Adjustments were made so that both the transducer and photomultiplier tube were at the proper focal distance from the jet's centerline. In practice, once the transducer was placed so that the beams crossed along the centerline, the PM tube was adjusted in a direction perpendicular to the centerline. The optimum distance from the beam crossing was the one that offered the sharpest image of the beam pairs in the PM tube "sight."

The beam pairs are not visible in the sight unless some transparent object (plexiglass, paper, etc.) is placed at the beam intersection. A circular, plastic disc driven by an electric motor served this purpose. With the disc rotating, further adjustment of the PM tube was possible by observing the validation rates achieved for given PM tube positions. With the proper alignment, validation rates in the range of 990 to 999 were obtained.

The rotating disc proved to be an excellent device for setting the alignment. The rotational speed (and hence

the tangential velocity at a given radius) was known and thus provided a check on the digital velocity presentation. Additionally, the best bandpass could be figured exactly, so that alignment was the only significant variable capable of producing unsatisfactory validation rates.

Strictly speaking, one other factor could have resulted in unacceptable validation rates: failure of the beam pairs to intersect properly. On the infrequent occasions that adjustments were made to the transducer, the possibility existed that beam alignment was changed.

Realignment of the beams was a simple operation. A beam expander (a small lens) placed at the approximate beam crossing point projected a set of fringe lines onto the wall. Strong, sharp fringes were obtained when the beams intersected properly, and weak or no fringes resulted with poor alignment.

In addition to serving the alignment function, the beam expander also provided a simple means to observe the extent of the vibrations present in the experimental location. With the transducer and expander on the isolated mounts, movements in the control room and smoke tunnel had no effect on ght fringes. If the mounts were tapped slightly, the fringe pattern became extremely unstable or disappeared altogether.

B. MEASUREMENTS OF NON-OSCILLATING JET FLOW

In order to make the jet stationary, the feedback loops were removed and modeling clay was used to seal the loop fittings. "Simultaneous" measurements with the pitot tube and the LDV were then taken by placing the pitot tube in the tunnel so that its dynamic pressure port was approximately 1 mm downstream of the laser beam intersection. The small difference in measuring locations should have had no observable effect on the velocities measured by the two methods.

The maximum distance from the centerline (in the $\pm$ y direction) for which measurements were possible was limited by the ability to detect changes in the water U-tube for the pitot tube case. LDV measurements were constrained by sparse seeding concentrations at "large" distances from the centerline. The LDV limitation could likely have been made less severe had additional particles been fed into the entrainment region near the jet exit. This could have been done with small smoke ejectors mounted on the exterior of the jet. It was not felt that the limitation was severe enough to warrant the additional effort, however.

LDV measurements were typically arrived at by recording approximately six velocity displays (from the mean

velocity computer) and averaging them to get the mean velocity for a given x, y point. An ENSEMBLE WIDTH of 256 or 4096 was generally used. Since mean velocities were desired, 4096 was the desired width, but 256 was used when delays in getting velocity updates from the mean velocity computer were excessive.

Special attention had to be given to those samples taken using an ENSEMBLE WIDTH of 1 due to the possibility of biasing errors. Displays obtained with larger widths received a bias correction by the mean velocity computer prior to display, and as such could be averaged in the normal manner:

$$\overline{U} = \frac{N_i \cdot v_i}{N_i}$$

where N_i is the number of samples of velocity v_i seen by the counter.

Such an averaging scheme if applied directly to the velocities of the ensemble group (which would be the case if applied to EW=1 data) would result in a "mean" value that was too high. This is due to the flow being sampled when a particle is present in the measuring volume, not randomly. Were a flow to fluctuate in a square wave fashion,

for instance, the velocity would be equal to U half the time and equal to zero the other half. Since no particles go through the measuring volume during the time in which the velocity is zero, and since the LDV can only measure velocities when particles are present, the only velocity seen will be U. Hence an "average" of U instead of U/2 would be computed.

If it is assumed that the sample time is sufficiently short and the particle density and size are uniform, then the probability of finding a particle in the measuring volume is proportional to the velocity of the flow. [9] This leads to the improved one-dimensional formula:

$$\overline{U} = \frac{N_i}{\frac{N_i}{v_i}}$$

To illustrate the difference in the two formulas, consider the following data table:

$v_1 = 10 \quad N_1 = 2$

$v_2 = 20 \quad N_2 = 2$

$v_3 = 30 \quad N_3 = 1$

$v_4 = 40 \quad N_4 = 3$

The first (biased) formula yields:

$$\bar{U} = \frac{2 \cdot 10 + 20 \cdot 2 + 30 \cdot 1 + 40 \cdot 3}{8} = 26.25$$

The second formula (with bias correction) yields:

$$\bar{U} = \frac{2 + 2 + 1 + 3}{\frac{2}{10} + \frac{2}{20} + \frac{1}{30} + \frac{3}{40}} = 19.59$$

As mentioned earlier, normal averaging yields a value which is too high, and as can be seen above, may be significantly different from the true value.

In addition to the mean velocity measurements, a series of turbulence factor calculations were made with the jet in the stationary mode. The turbulence factor (TF) is a measure of the amount the velocity fluctuates at a given point in the flow. For jets, the TF used is the standard deviation of the velocity at a given point in the flow, nondimensionalized by the centerline velocity of the jet:

$$TF = \frac{\sigma}{\bar{U}_c} = \frac{\sqrt{\sum_{i}^{N} \frac{(U_i - \bar{U})^2}{N-1}}}{\bar{U}_c}$$

where N is the number of velocity samples taken at the point, $\bar{U}$ is the unbiased mean of the samples at the point, and U_c is the mean centerline velocity.

As mentioned in an earlier section, an ENSEMBLE WIDTH of 1 was used to generate the velocities from which the standard deviation was calculated.

In order to get an estimate of the extent to which factors peculiar to the manner in which the LDV system produces velocity data might affect the TF, the measurements were made on the rotating plastic disc. It was felt that this would present an extremely "laminar" flow with a minimal turbulence level. This was in effect, an ideal case to which other TF determinations could be referenced.

C. MEASUREMENTS OF OSCILLATING JET FLOW

Mean velocity calculations for this case were carried out in the same manner as for the non-oscillating jet. The primary difference, of course, was that the feedback loop was connected. Although devices of this sort are generally run at high air supply pressures, a maximum of two inches of mercury was used. This was due to the presence of excessive amounts of water in the air at higher pressures. At those pressures the water tended to collect in the feedback loops and drip from the nozzle exit as well.

Mean velocity data was obtained by the same simple averaging approach used in the non-oscillating case using

ensemble widths greater than 1. Once velocities were calculated for each of the measurement points, they were plotted using a Hewlett-Packard 9830 computer equipped with a plotter unit.

Curve fits for the points plotted were obtained by using the polynomial regression portion of the Plotter Pac cassette tape. The Hewlett-Packard system provided an excellent means of getting a good quality plot with a minimum of time and effort. Time savings were especially great when turbulence factors were calculated and plotted. Modifications to the basic Plotter Pac programs were easily made, and special function keys used to tailor the programming to the specific needs of the data and output requirements.

Instantaneous "strobing" measurements were made with the jet attached to the bottom wall. This was accomplished by attaching the pressure transducer near the nozzle exit on the same side (bottom side) as the wall to which the jet would be attached during the measurements. To make measurements of velocities while the jet was attached to the top wall, the transducer could have been attached to the upper, front side of the jet.

The pulse generator was set with virtually no delay (see Figure 2) between the pressure transducer's triggering input and the generation of the pulse which tripped the counter. Thus, velocities were measured only while the jet was attached to the bottom wall. Velocities at the various x, y points were not measured simultaneously, of course, but were made at identical times during the jet's cycle. The consistency of the jet's period is shown in Figure 19 which is a photograph of the pressure transducer's output. The peaks on which the pulse generator is triggered are especially prominent.

Measurements with the jet in other orientations were not made, primarily due to lack of time available for conducting the experiments. A secondary consideration was the life time of the pressure transducer. The transducer's fatigue life on the order of 10^6 cycles is exceeded rather quickly by a jet with an oscillatory frequency of approximately 100 Hz.

VII. EXPERIMENTAL RESULTS

A. MEAN VELOCITY MEASUREMENTS OF NON-OSCILLATING JET

Mean velocity surveys of the non-oscillatory jet are shown graphically in Figures 20 through 23. Agreement between the LDV and pitot methods was good as can be seen in Figure 21. A companion thesis, Reference 10, showed that nondimensionalized plots of the same data were in excellent agreement with theory and other published results. Velocity measurements near the jet boundary were limited by the concentration of seeding particles, in the case of the LDV, and by difficulty in reading small water heights in the U-tube manometer, in the case of the pitot tube.

Profiles were taken at distances of 15 and 40 cm downstream of the nozzle and at reservoir pressures of 1, 2, and 3 inches of mercury. As predicted by theory, the familiar bell-shaped curve resulted in all cases, with absolute values of the velocities increasing with increasing pressure. The curve was not symmetric about the x-axis, however. This offset was due to the jet remaining attached to one exit wall. This tendency was also detected in Reference 9 by means of holograms.

B. TURBULENCE INTENSITY MEASUREMENTS

As seen in Figures 24 and 25, turbulence factors on the order of .01 to .03 were obtained for the rotating disc and the non-oscillating jet. For the disc, the value of approximately .015 is most meaningful, as that was the value at a radius of 3 inches, and the rotational velocity at that location was used to nondimensionalize the turbulence factor. The relatively large values of turbulence factor at smaller radii was due to this method of nondimensionalization.

The magnitudes of the turbulence factors are in agreement with those described in Reference 3 for a similar flow.

C. MEAN VELOCITY MEASUREMENTS OF THE OSCILLATING JET

Figures 26 and 27 show the results of simultaneous pitot and LDV surveys at downstream distances of 15 and 40 cm, respectively. These results show the double peak velocity reported in Reference 11. As indicated previously, the jet attaches to either exit wall for a brief period of time, and produces the peaks in the profile during the attachment portion of the cycle. The fact that one peak is larger than the other is an indication that the jet

remains attached to one wall longer than to the other. This bias is due, most likely, to the basic construction of the fluidic element which controls the oscillations.

The figures indicate that the peaks move farther apart as distance from the exit increases. This phenomenon is due to the spreading of the jet, and may be thought of as a divergence of two velocity vectors originating at the exit plane of the nozzle, according to Reference 7.

The mean velocity in the y-direction is shown in Figure 28. The double peak profile is seen once again for the same reasons that peaks were seen in the x-component profile.

D. INSTANTANEOUS VELOCITY MEASUREMENTS OF THE OSCILLATING JET

Instantaneous measurements were very adversely affected by an inability to maintain acceptable validation rates during the surveys. Using a counter-enabled window (Figure 2) of approximately 15 milliseconds and a delay time (between pressure trigger and counter enabled) of 10 nano-seconds, validation rates did not exceed 80. This was a significant problem as validation rates are a primary means of determining if the proper bandpass is being used.

Validation rates were poor due to the inhibiting of the counter operation while measuring an inherently turbulent

flow. As explained earlier, the counter requires at least eight consecutive fringe crossings before information can be passed to the mean velocity computer for a velocity calculation. In a turbulent flow many slant entries into the measuring volume can be expected, so generally more than one such set of eight fringe crossings will be needed. This effect, combined with the pressure signal's interruption of the normal counter operation, resulted in low validation rates.

An instantaneous velocity survey was made at x=15 cm, and p=2 inches of mercury with the inhibit parameters mentioned above. Two bandpass combinations were used during the survey. Both used LOW PASS settings of 100 MHz, and HIGH PASS settings of 4 MHz and 16 MHz. Other combinations were attempted, but no velocity updates were obtained. The 100/16 combination resulted in velocity measurements of approximately 43 meters per second at all measuring locations between -10 and +7 centimeters in the y-direction. Using the 100/4 combination velocities of approximately 14 meters per second resulted for all locations.

Due to the inadequate validation rates, it is not clear which value of velocity was appropriate for a given location. The data do suggest, however, that the instantaneous

flow field consists of a high velocity region around the jet's instantaneous centerline and a lower, relatively uniform velocity field elsewhere. This is essentially what would be expected if a Gaussian velocity profile were superimposed on the instantaneous jet centerline, and allowances were made for mixing effects (due to the oscillation) on the edges of the profile.

VIII. CONCLUSIONS

The laser Doppler velocimeter was found to be readily adaptable to the problem of making mean velocity measurements of an oscillating or non-oscillating jet. The primary limitation in such measurements was found to be the concentration of seeding particles, which decreased in the transverse and axial directions. Additional seedings of the entrained air should permit measurements at increased transverse distances from the jet centerline.

Instantaneous velocity measurements were found to be most difficult due to the low validation rates which were obtained. To obtain improved measurements, the validation rates must be improved to ensure that proper bandpassing is being utilized. It is concluded that such improvements would permit the laser Doppler velocimeter to make the cyclic velocity measurements without the use of the flow perturbing apparatus that accompany more conventional techniques.

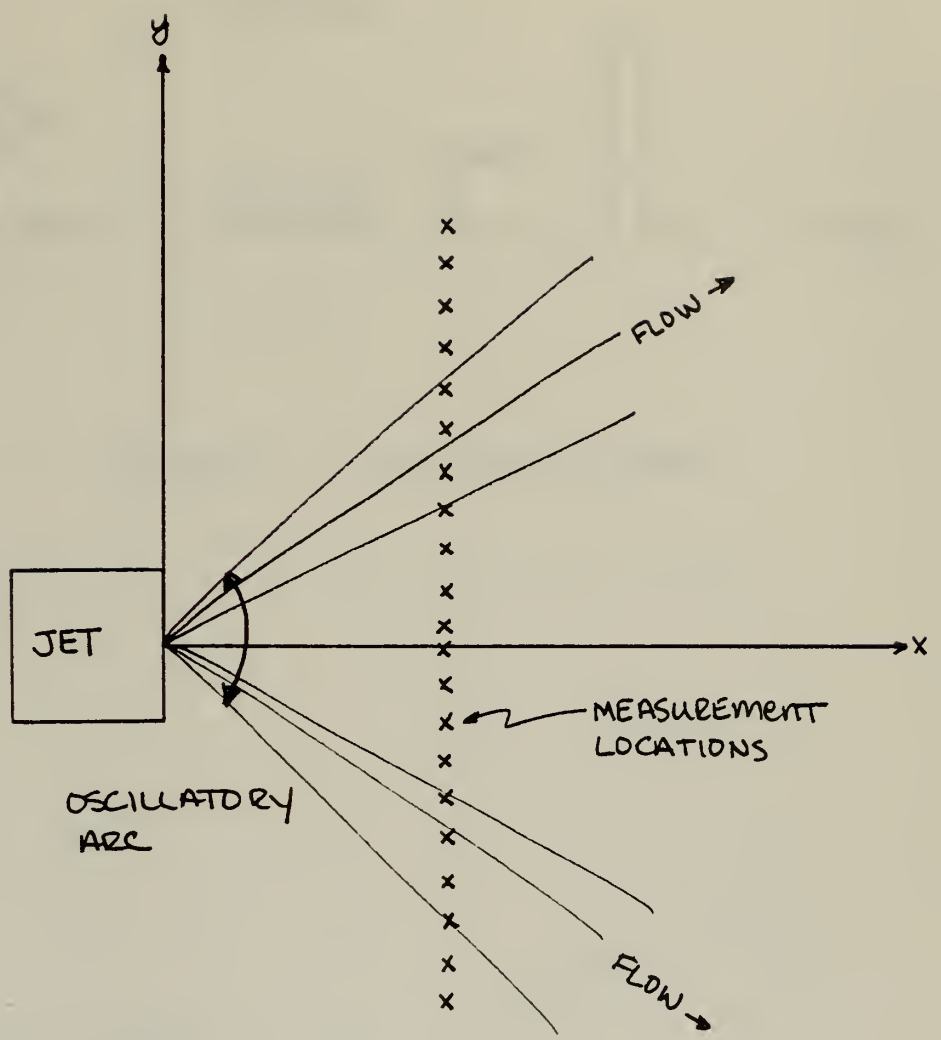

FIGURE 1. GRID SYSTEM

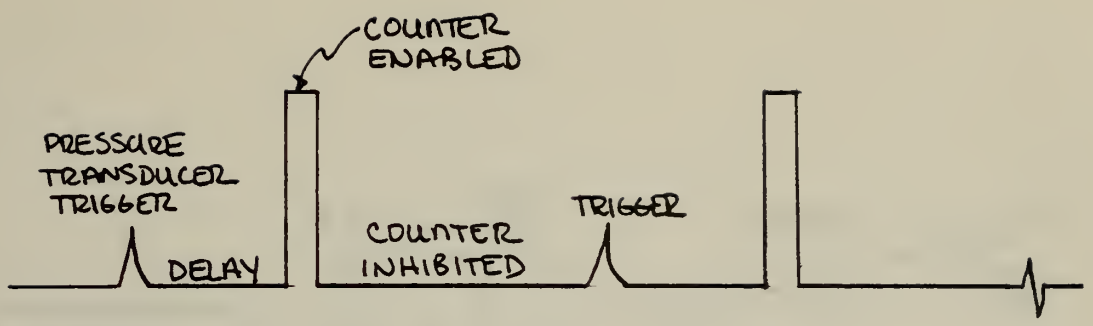

FIGURE 2. COUNTER CONTROL

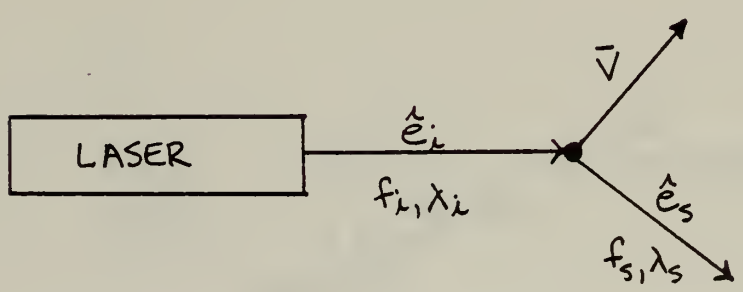

FIGURE 3. LIGHT SCATTERING

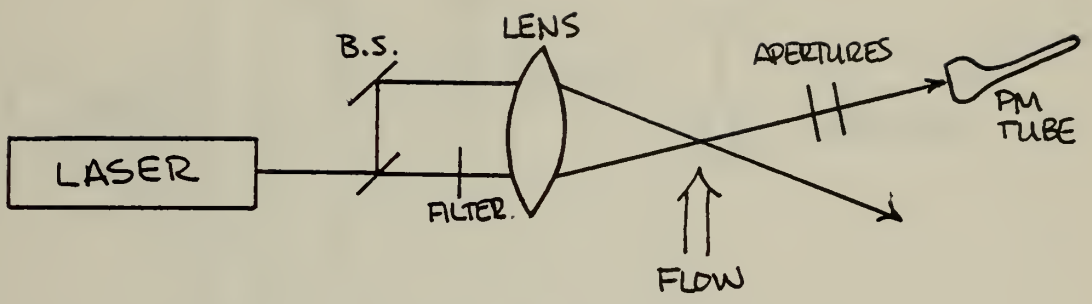

FIGURE 4a. REFERENCE BEAM SETUP

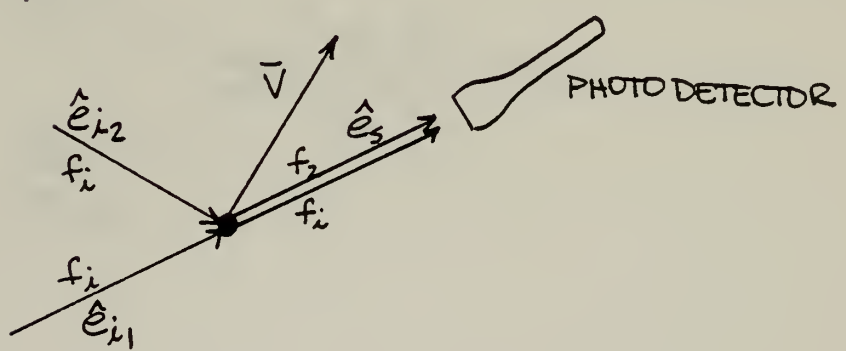

FIGURE 4b VECTOR DIAGRAM

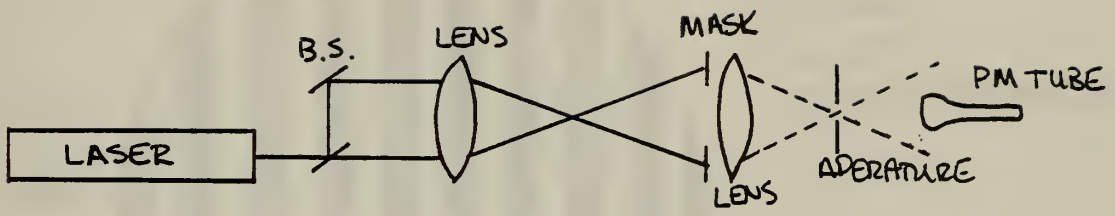

FIGURE 5a. DUAL SCATTER SETUP

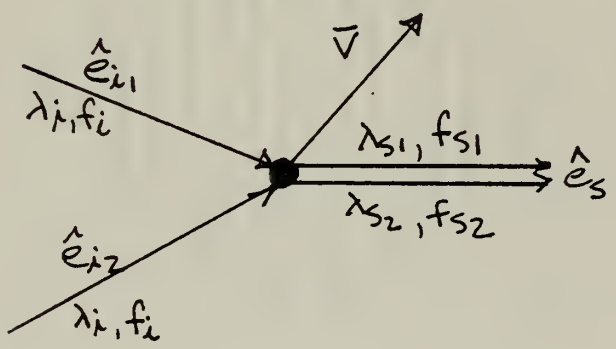

FIGURE 5b. VECTOR DIAGRAM

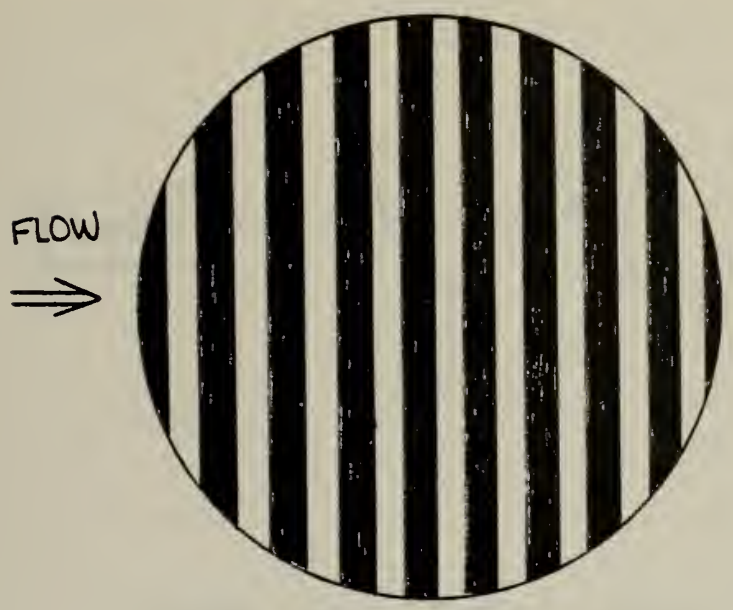

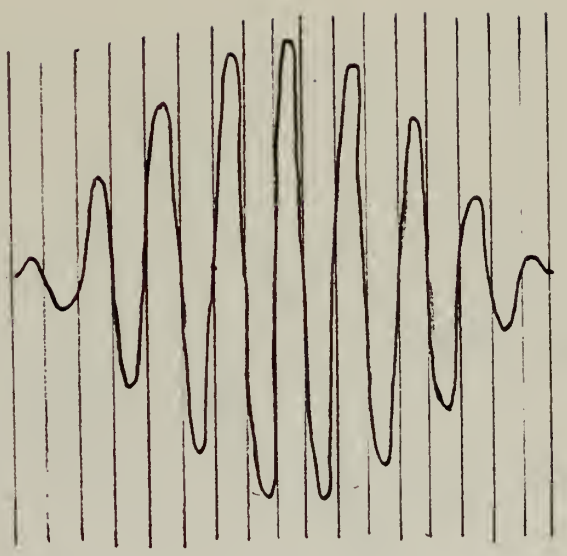

FIGURE 5c. FRINGE MODEL

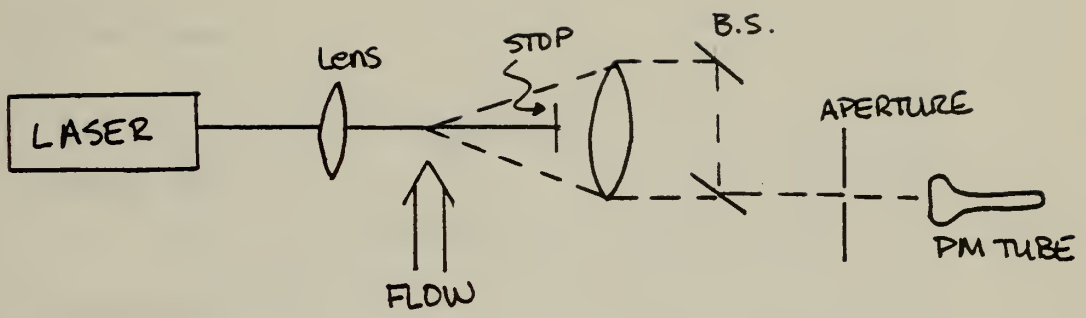

FIGURE 6a. SINGLE BEAM SETUP

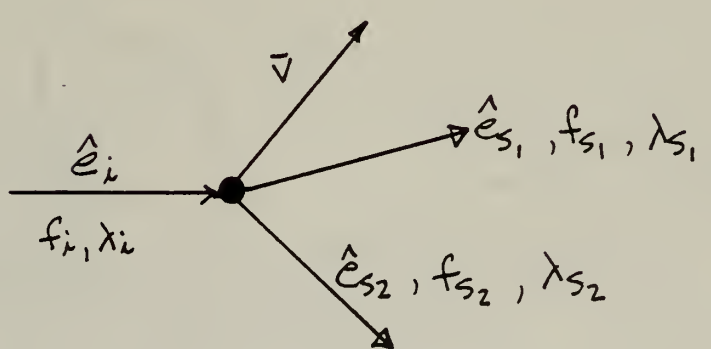

FIGURE 6b. VECTOR DIAGRAM

FIGURE 7a. FEEDBACK PORTS CLOSED

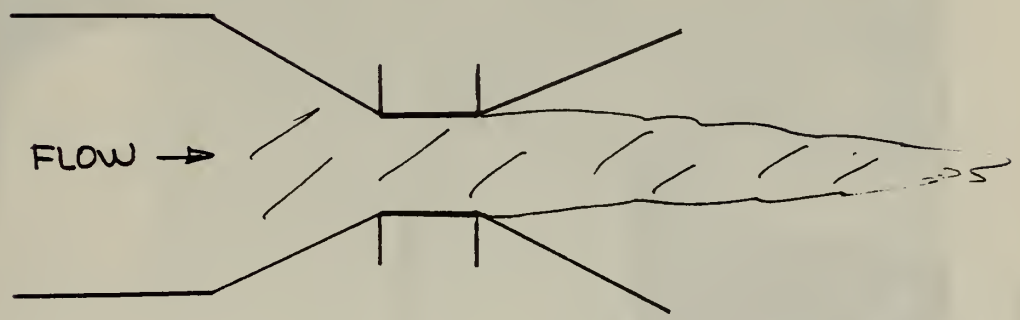

FIGURE 7b. FEEDBACK PORTS OPEN

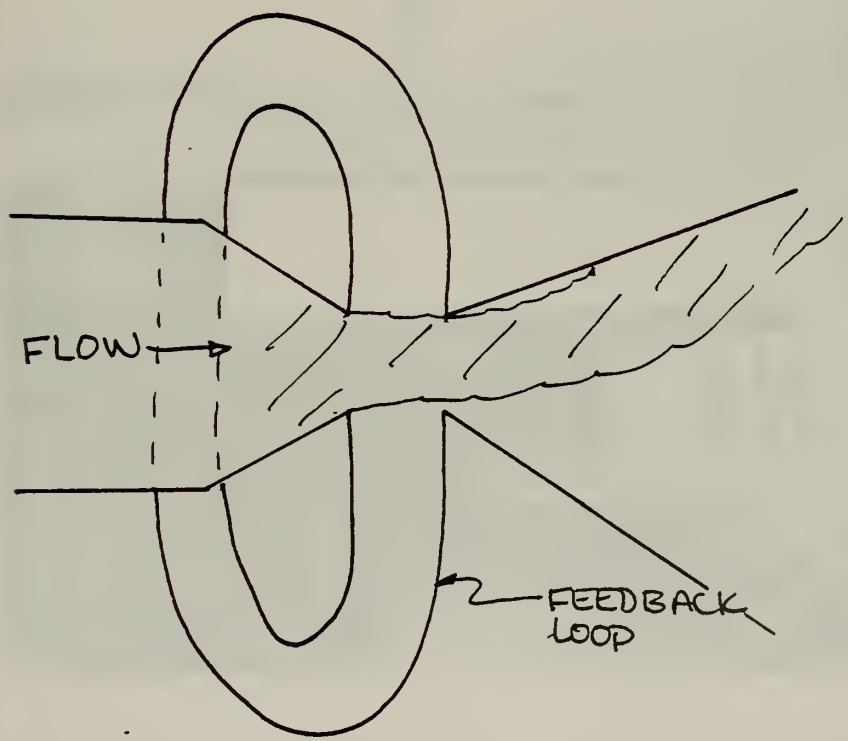

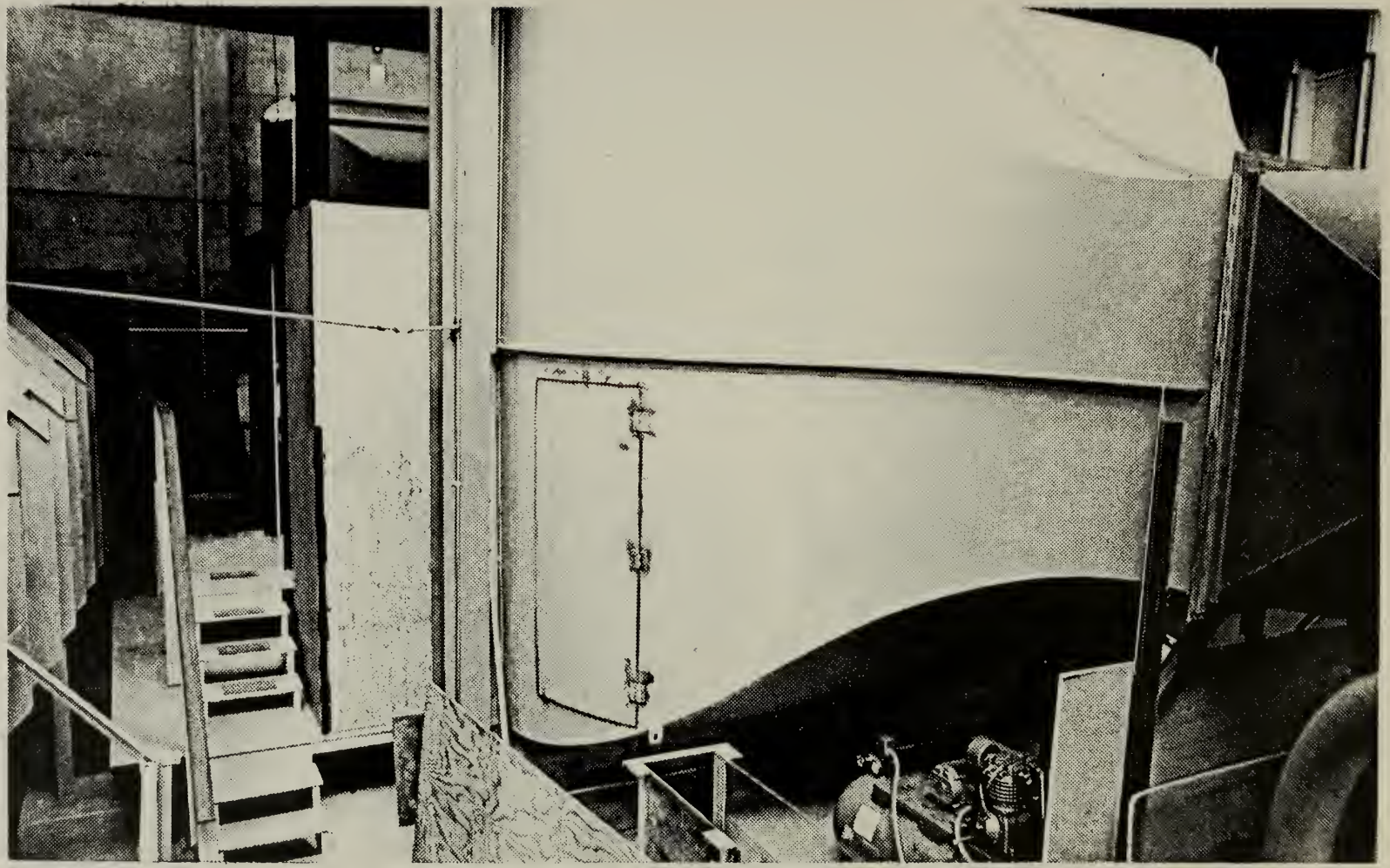

Figure 8. Smoke Tunnel and Control Room

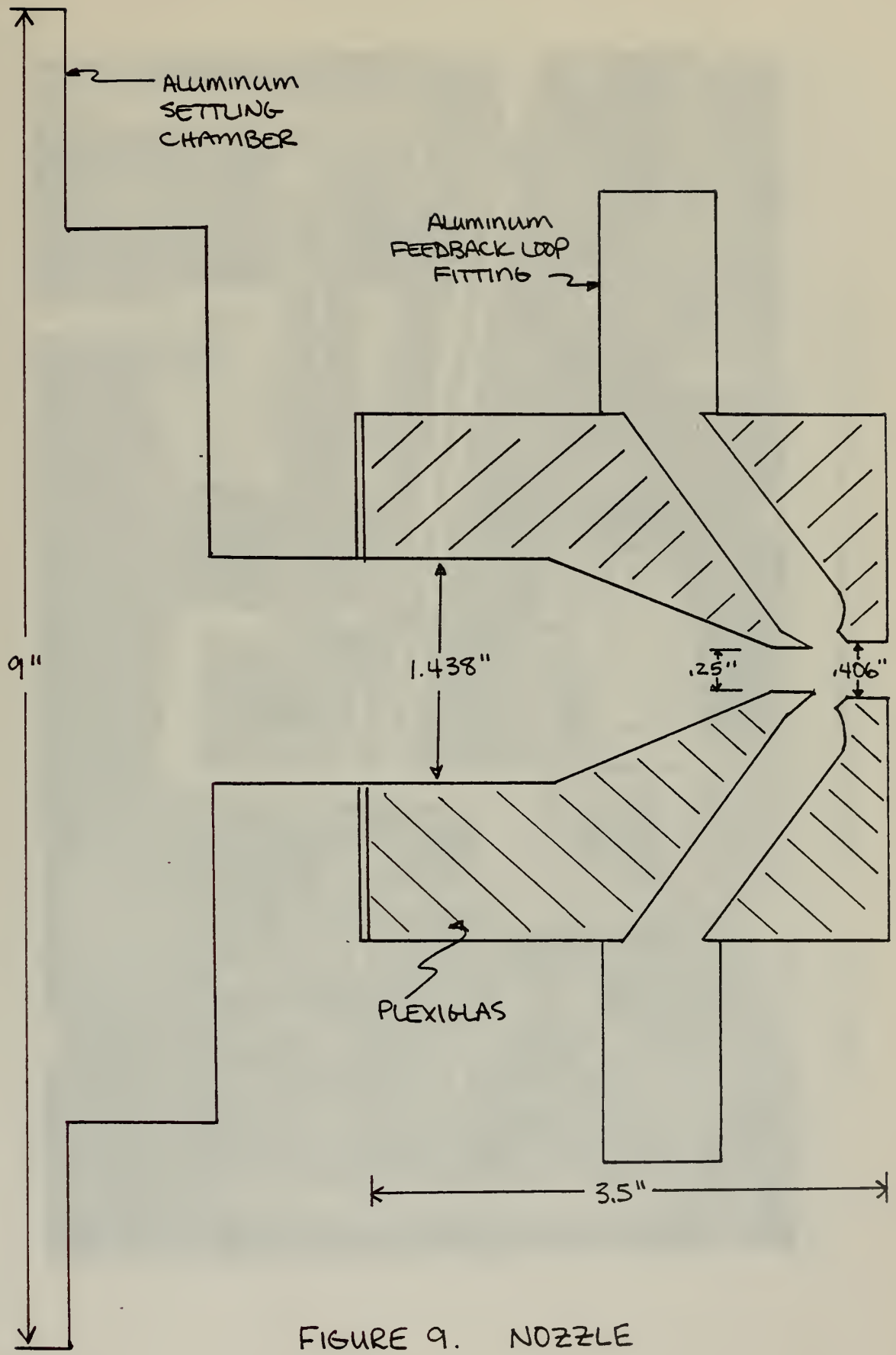

FIGURE 9. NOZZLE

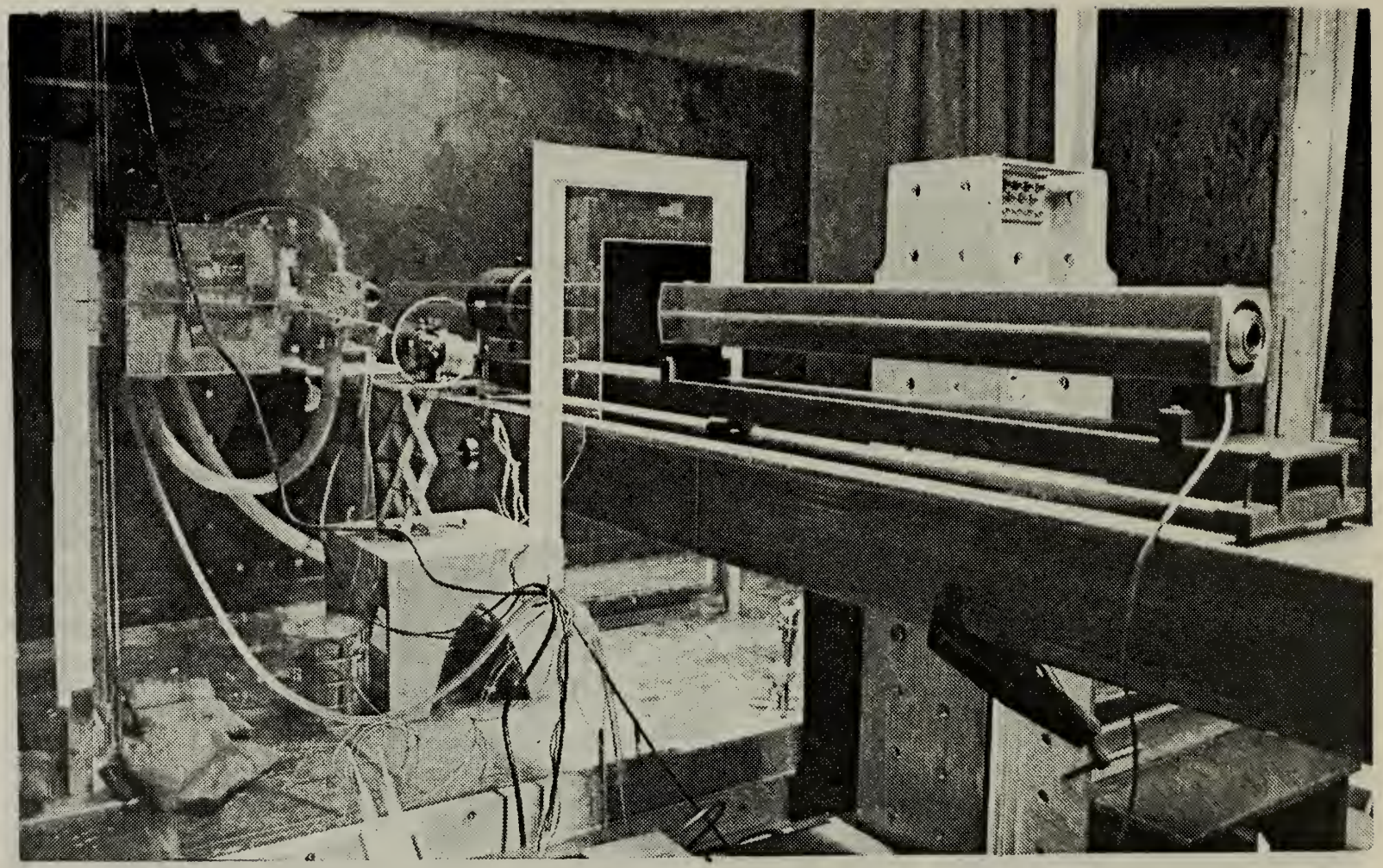

Figure 10. Settling Chamber, Nozzle, and LDV Optics

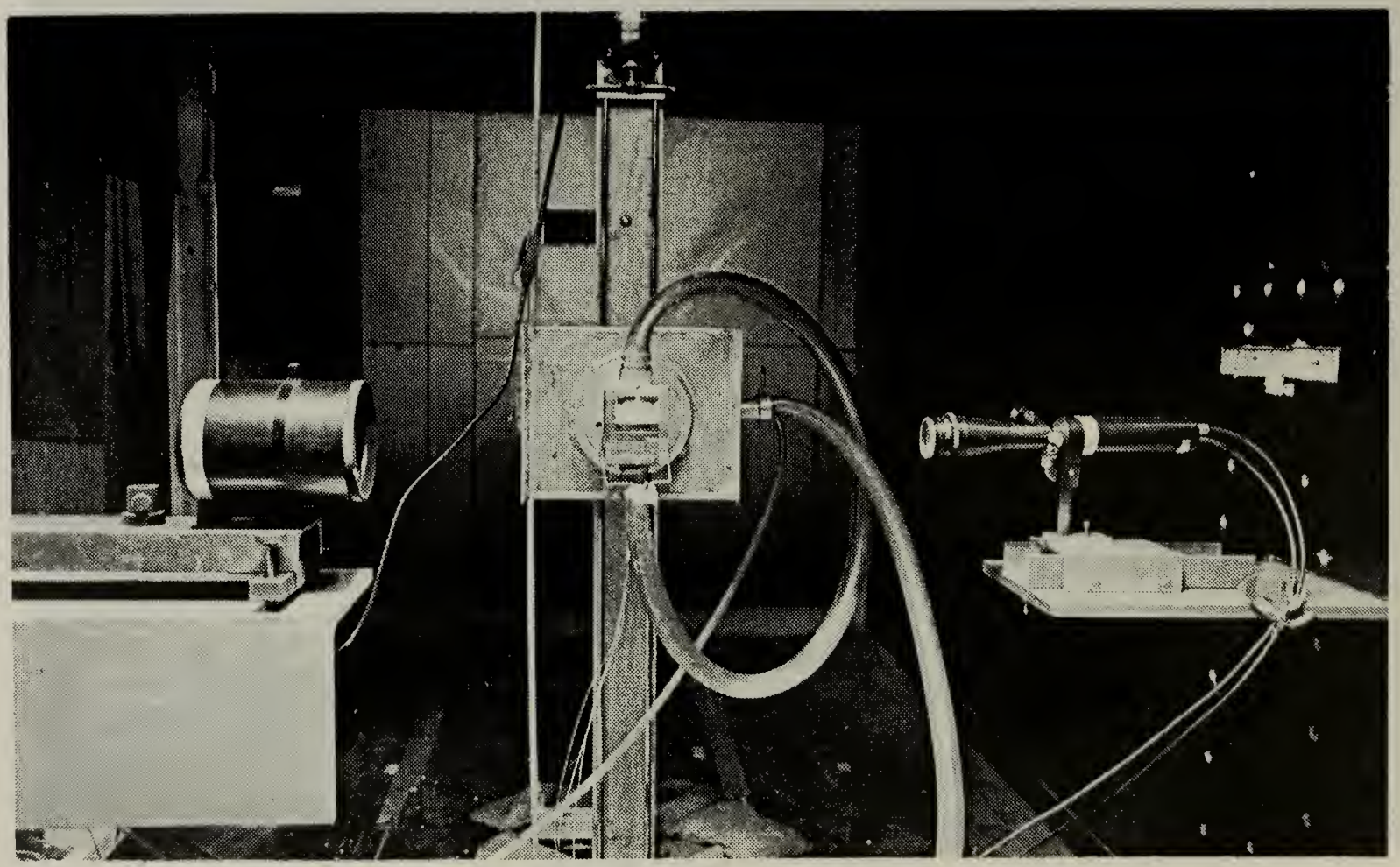

Figure 11a. Nozzle Mounted on Traversing Mechanism

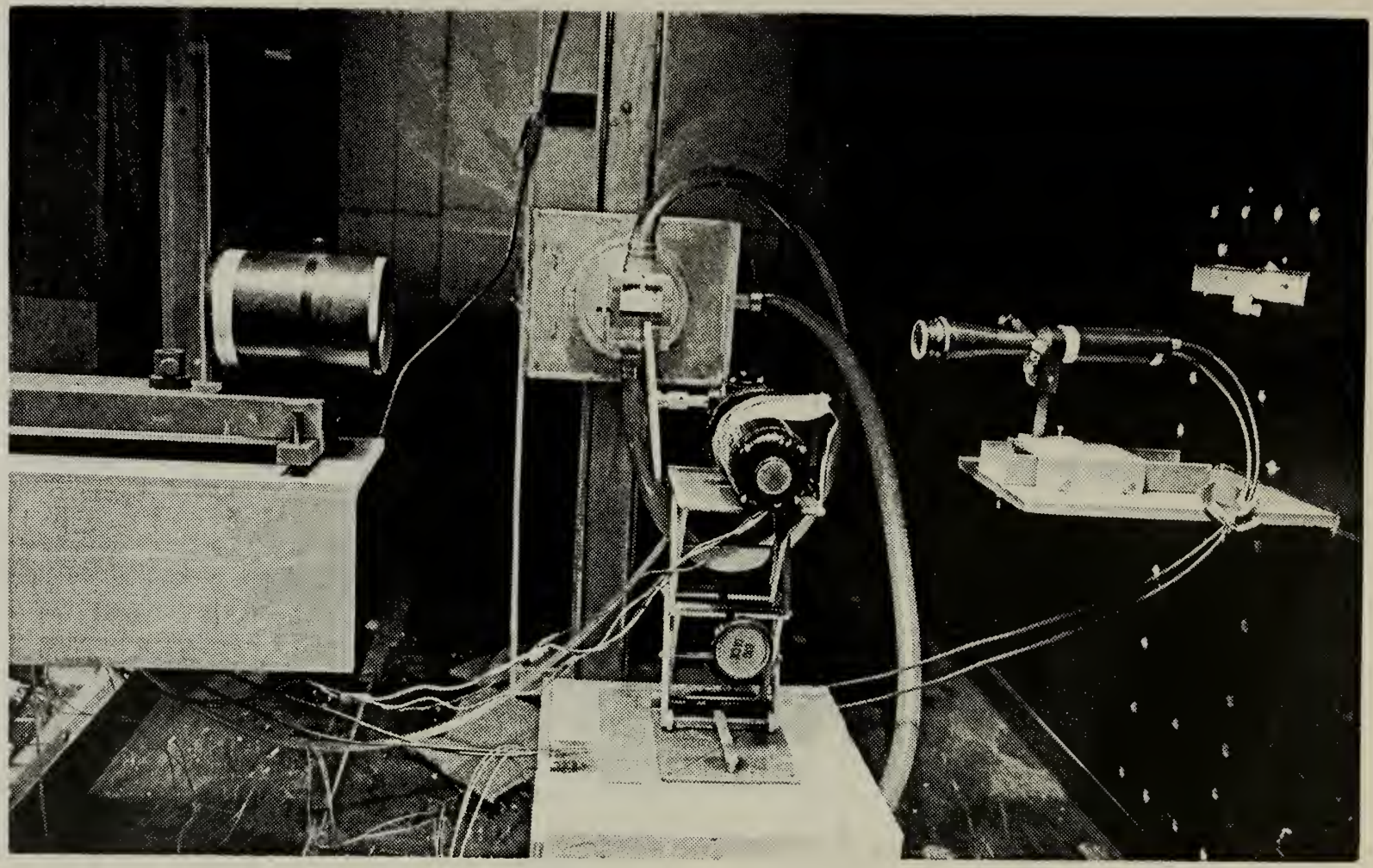

Figure 11b. Arrangement With Rotating Disc in Position

FIGURE 12. SUPPORT ASSEMBLY

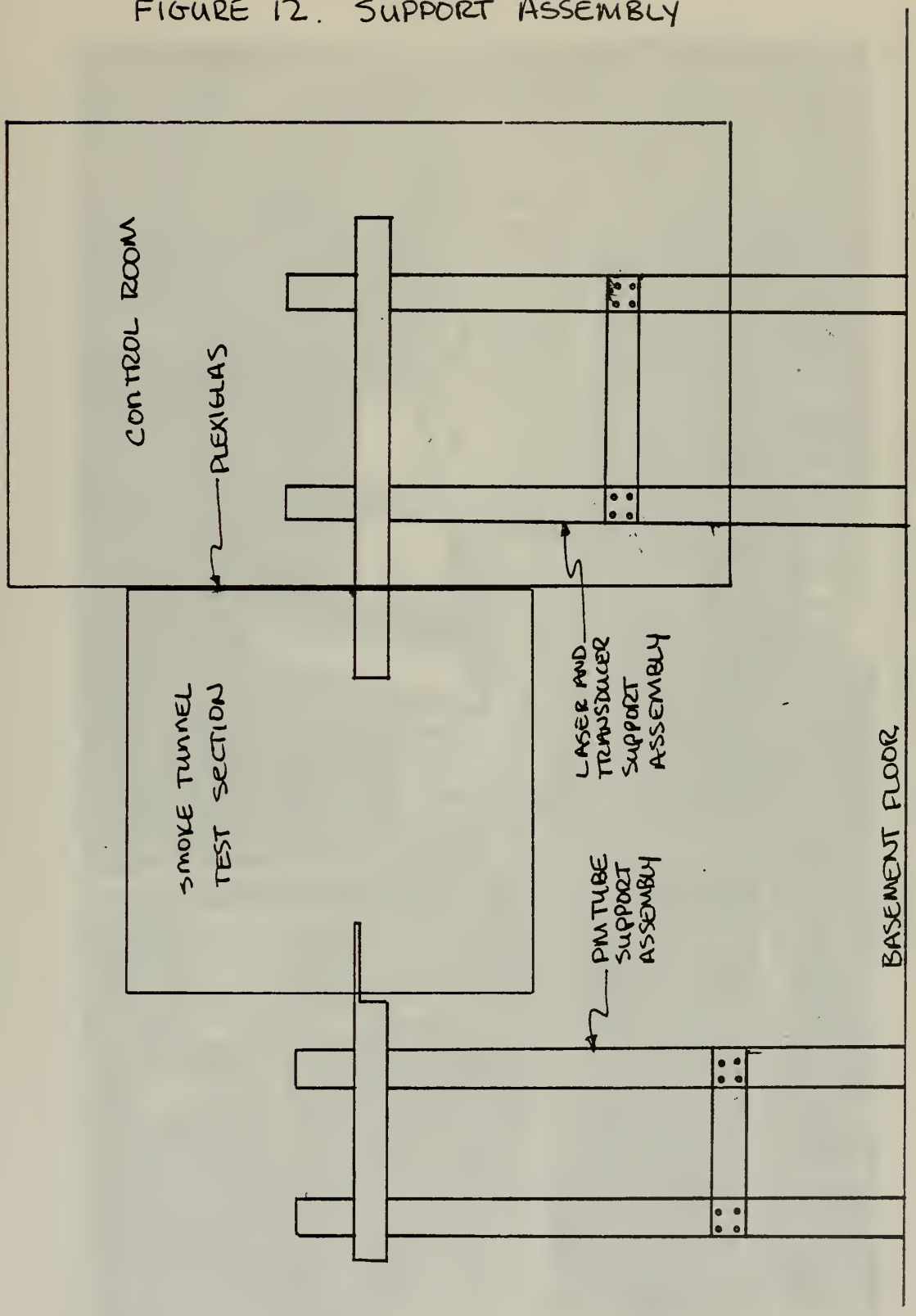

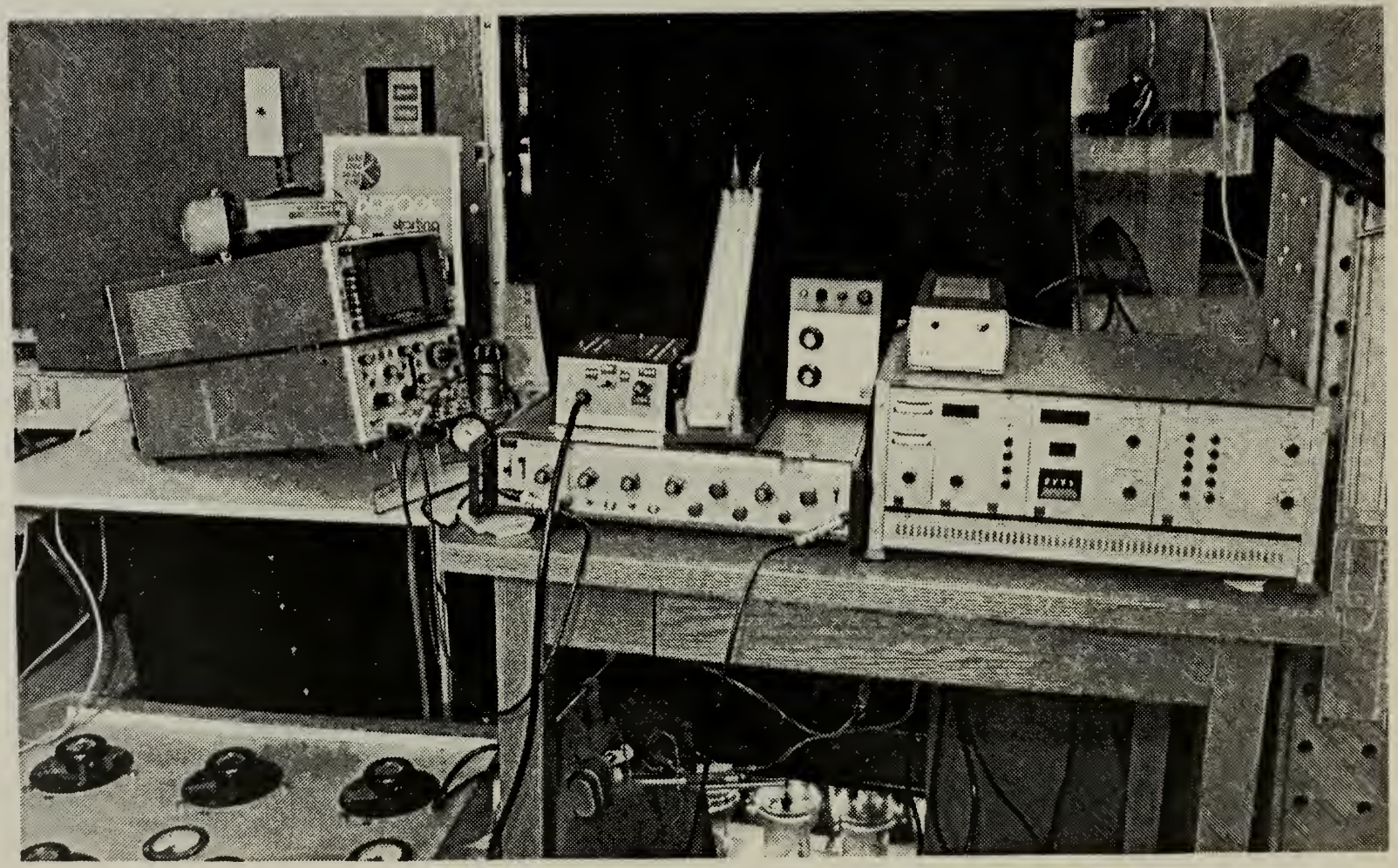

Figure 13. Control Room Components

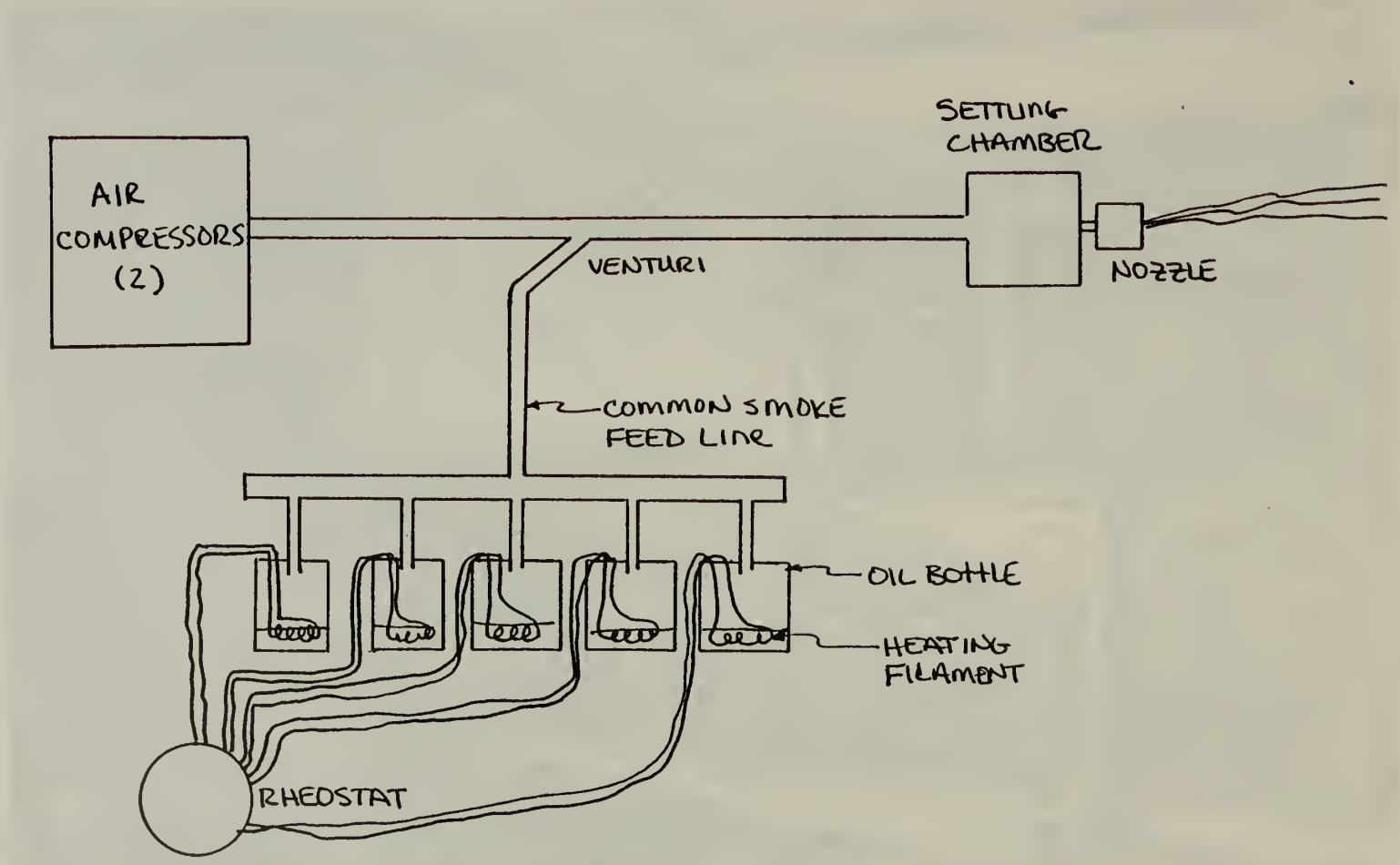

FIGURE 14a. PARTICLE GENERATION

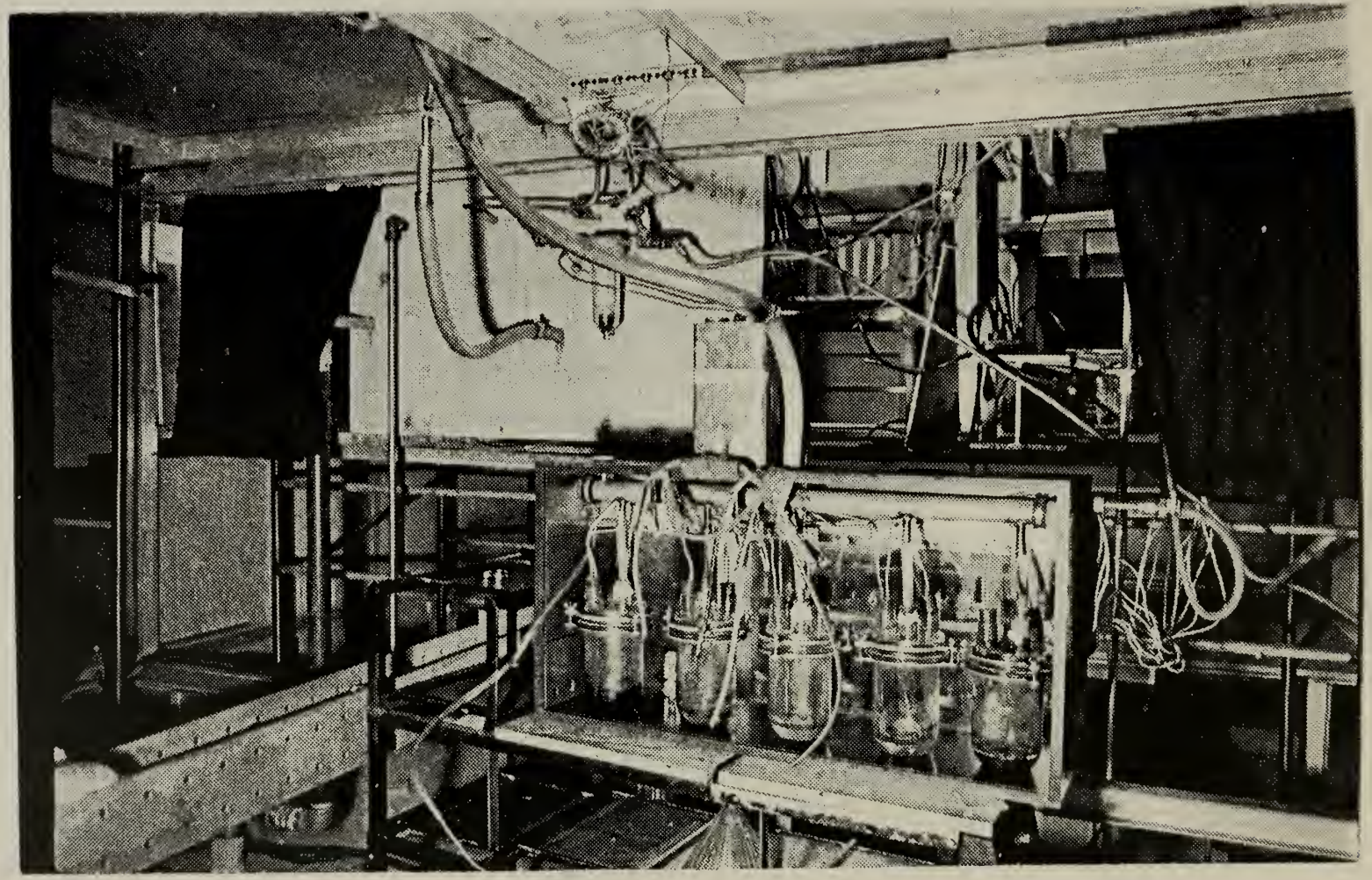

Figure 14b. Particle Generator

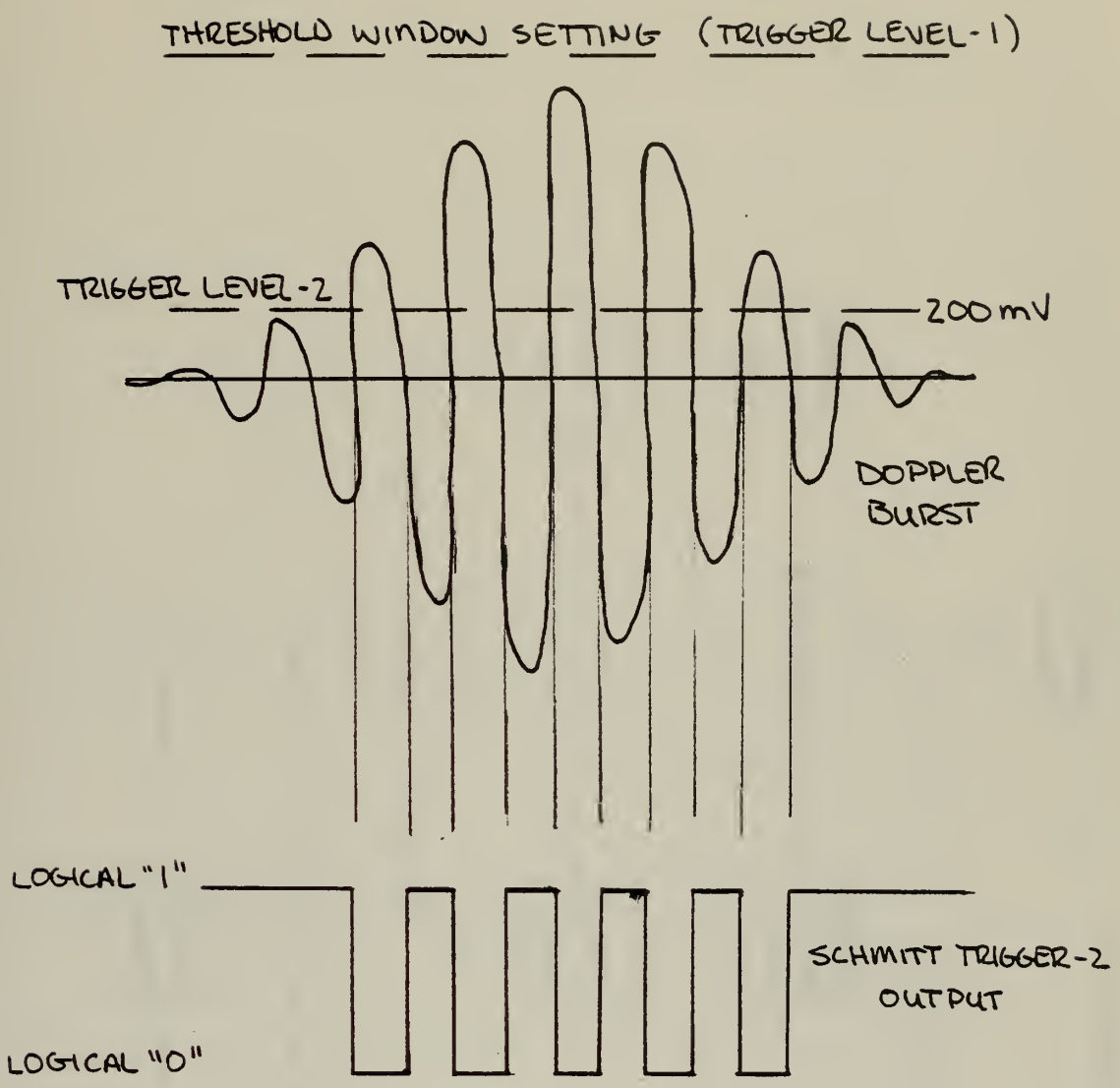

LOGICAL "0" when SIGNAL exceeds 200mV
LOGICAL "1" when VOLTAGE PASSES THROUGH ZERO

FIGURE 15. DETECTION OF FRINGE PASSAGE

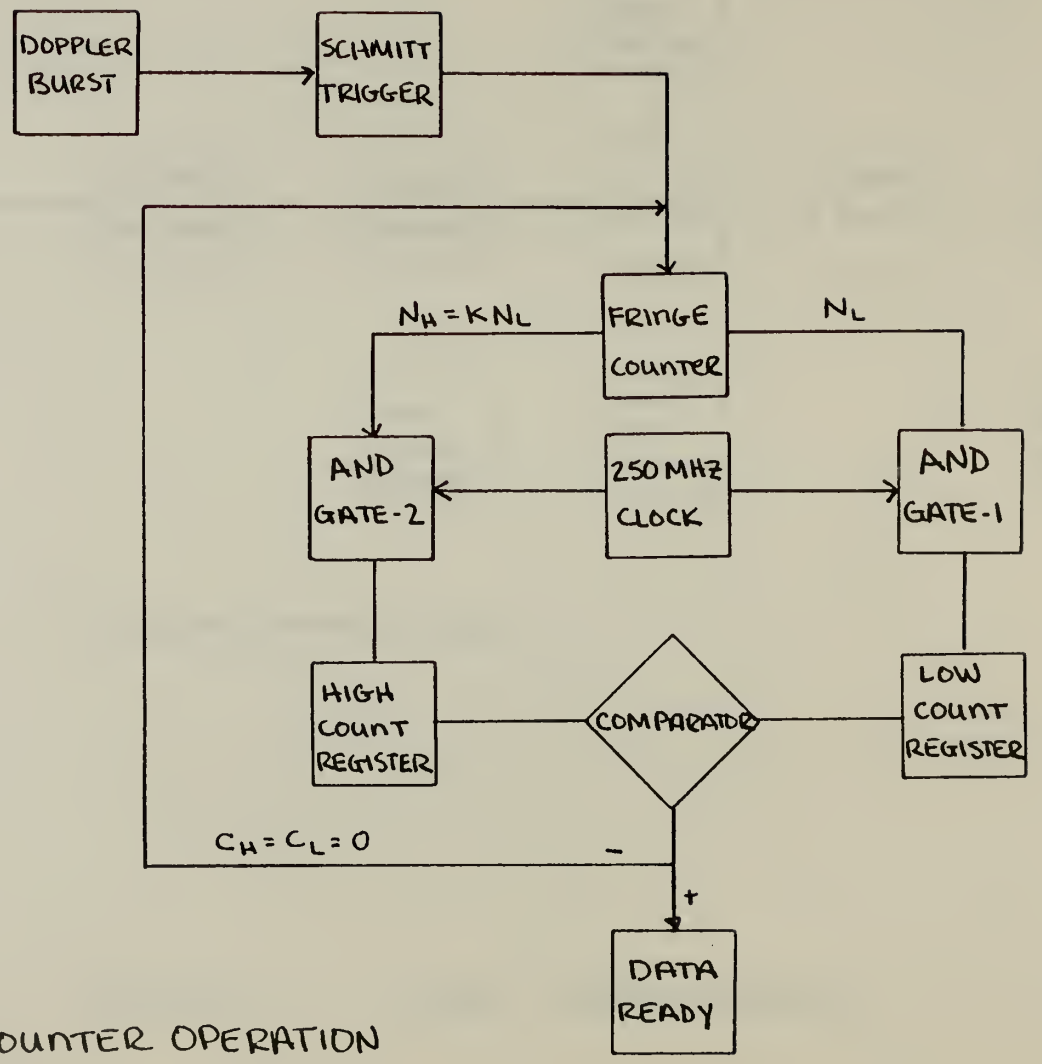

FIGURE 16. COUNTER OPERATION

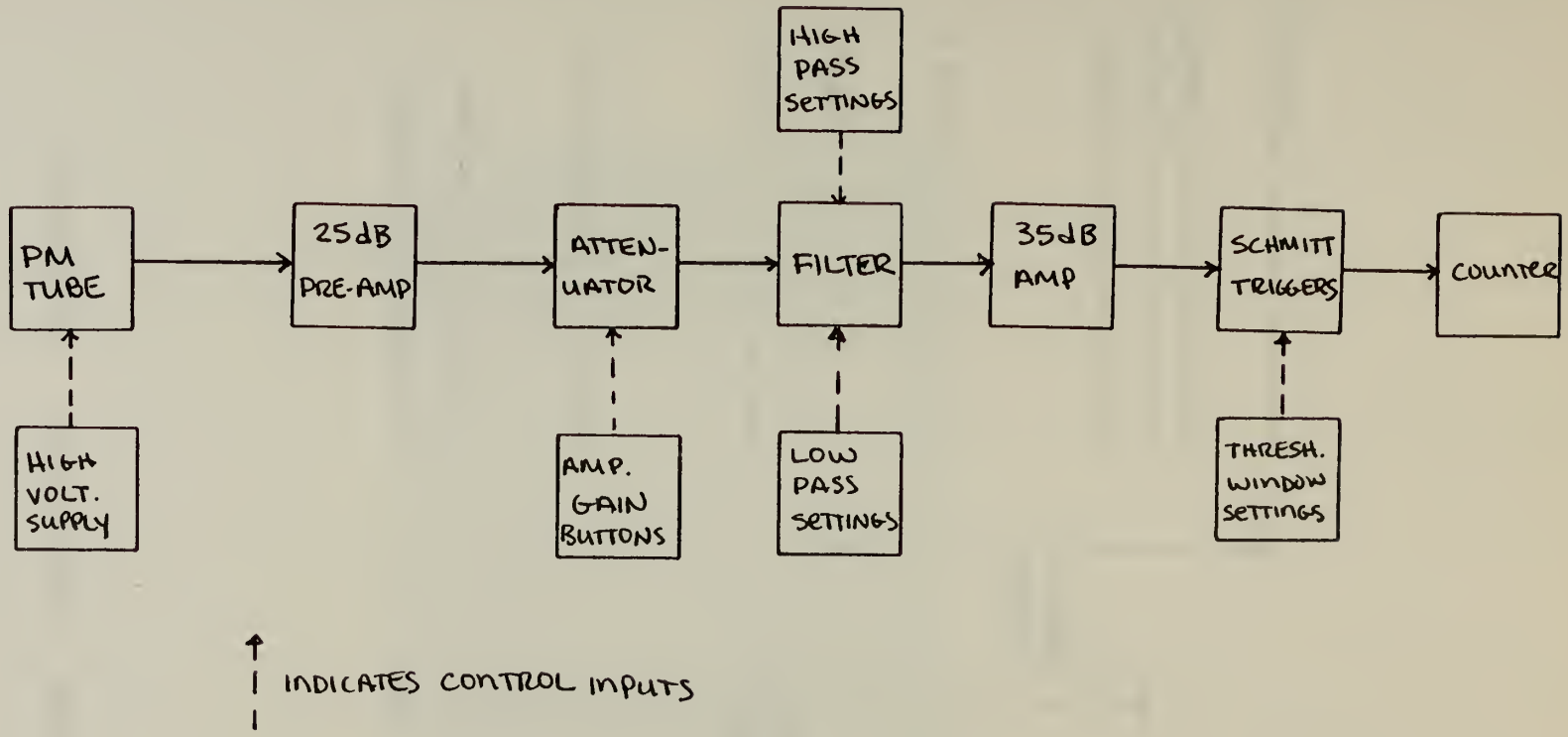

FIGURE 17. SIGNAL CONDITIONING

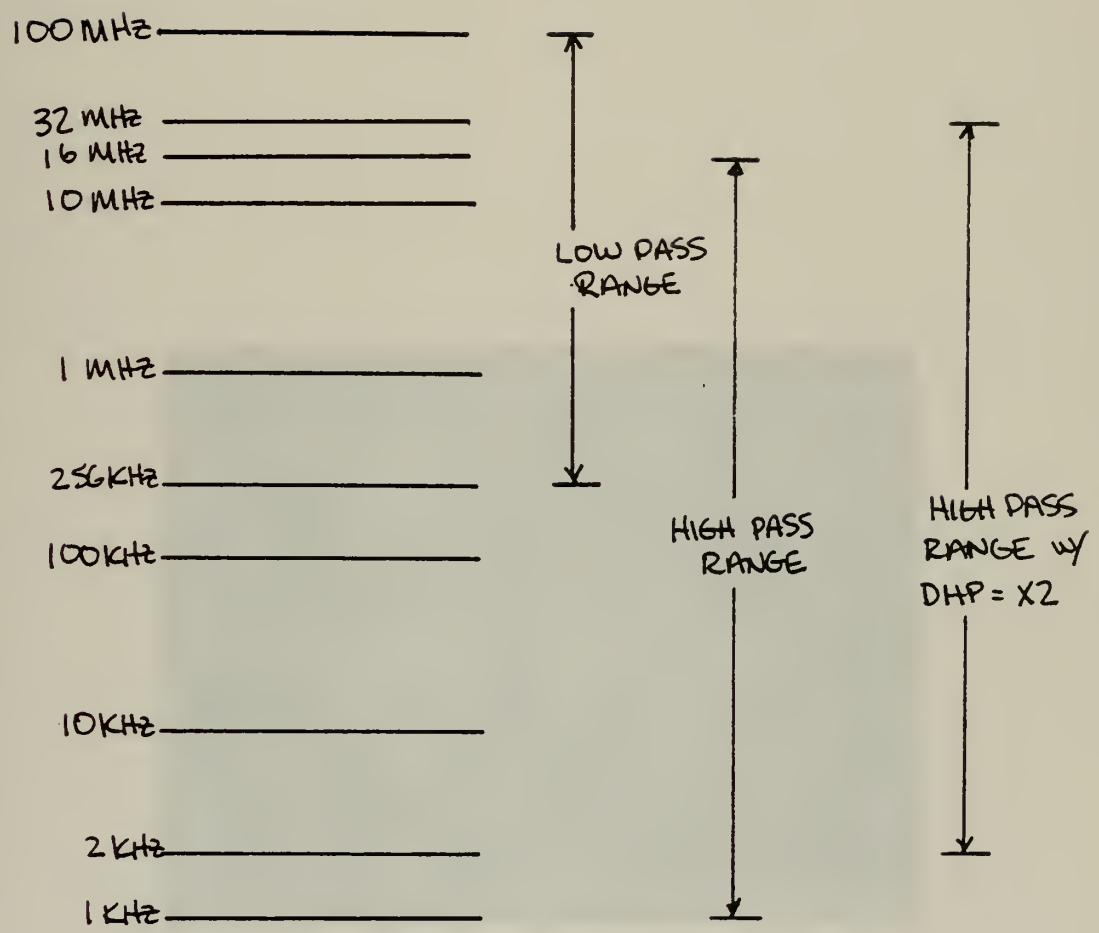

FIGURE 18. BANDPASS RANGE

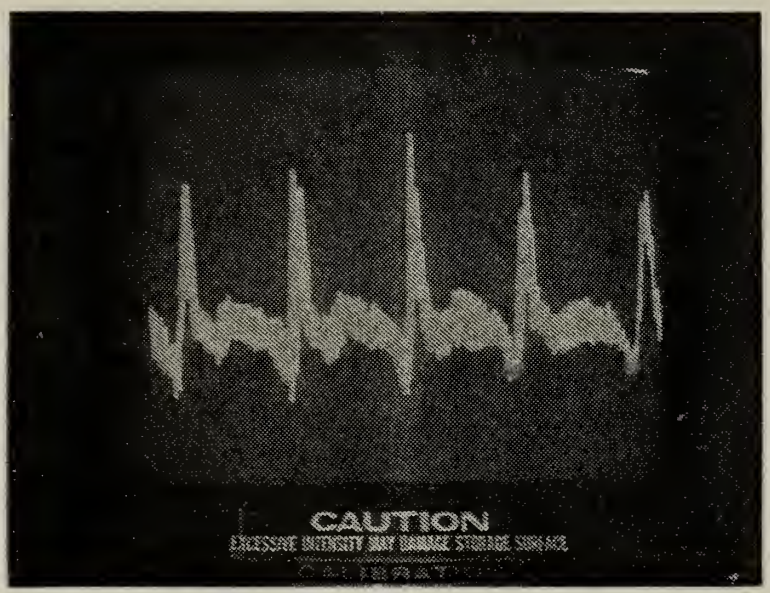

Figure 19. Output of Pressure Transducer

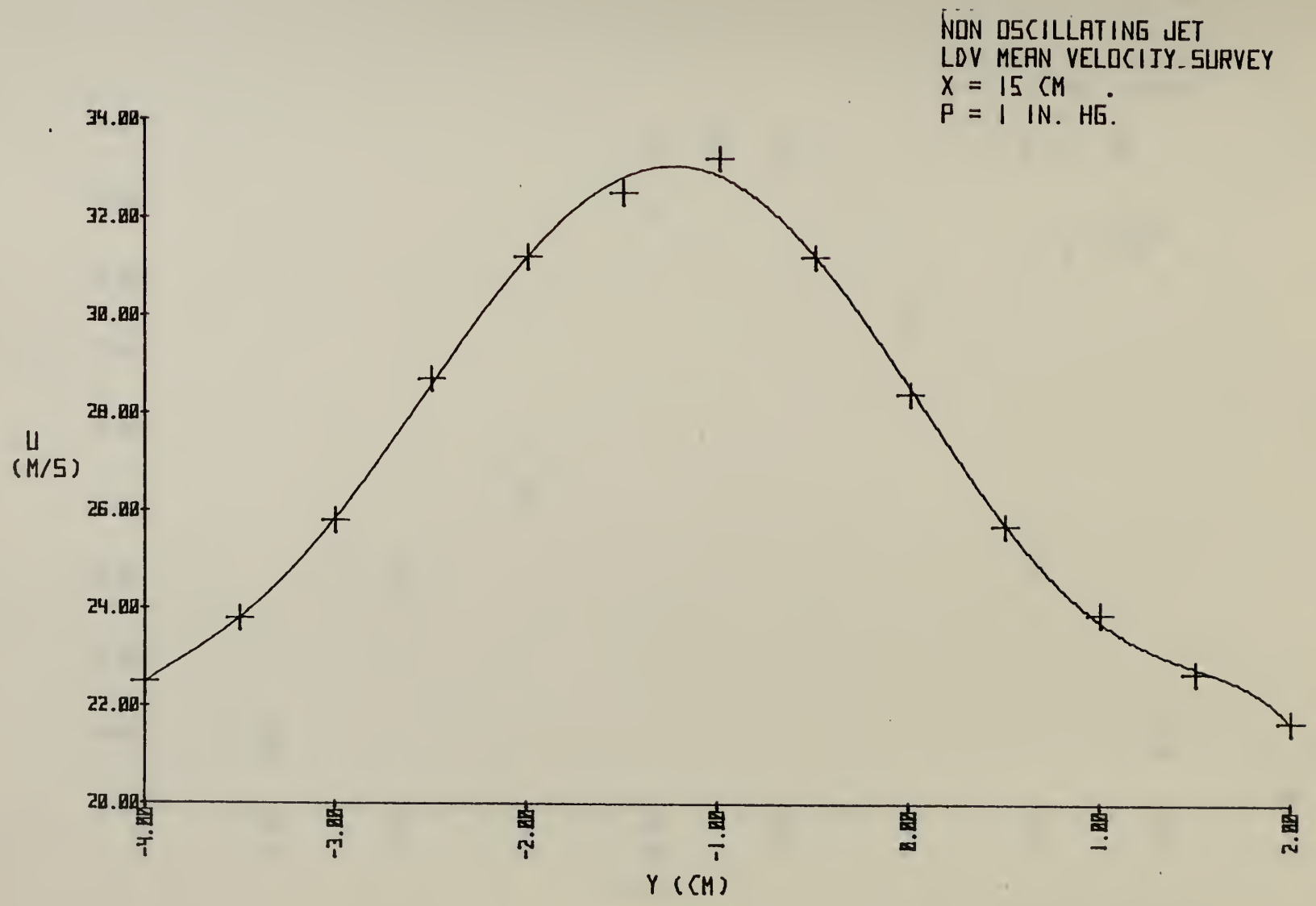
NON OSCILLATING JET
LDV MEAN VELOCITY SURVEY
X = 15 CM
P = 1 IN. HG.
U
(M/S)
34.00
32.00
30.00
28.00
26.00
24.00
22.00
20.00
-4.00
-3.00
-2.00
-1.00
0.00
1.00
2.00
Y ((M)

FIGURE 20

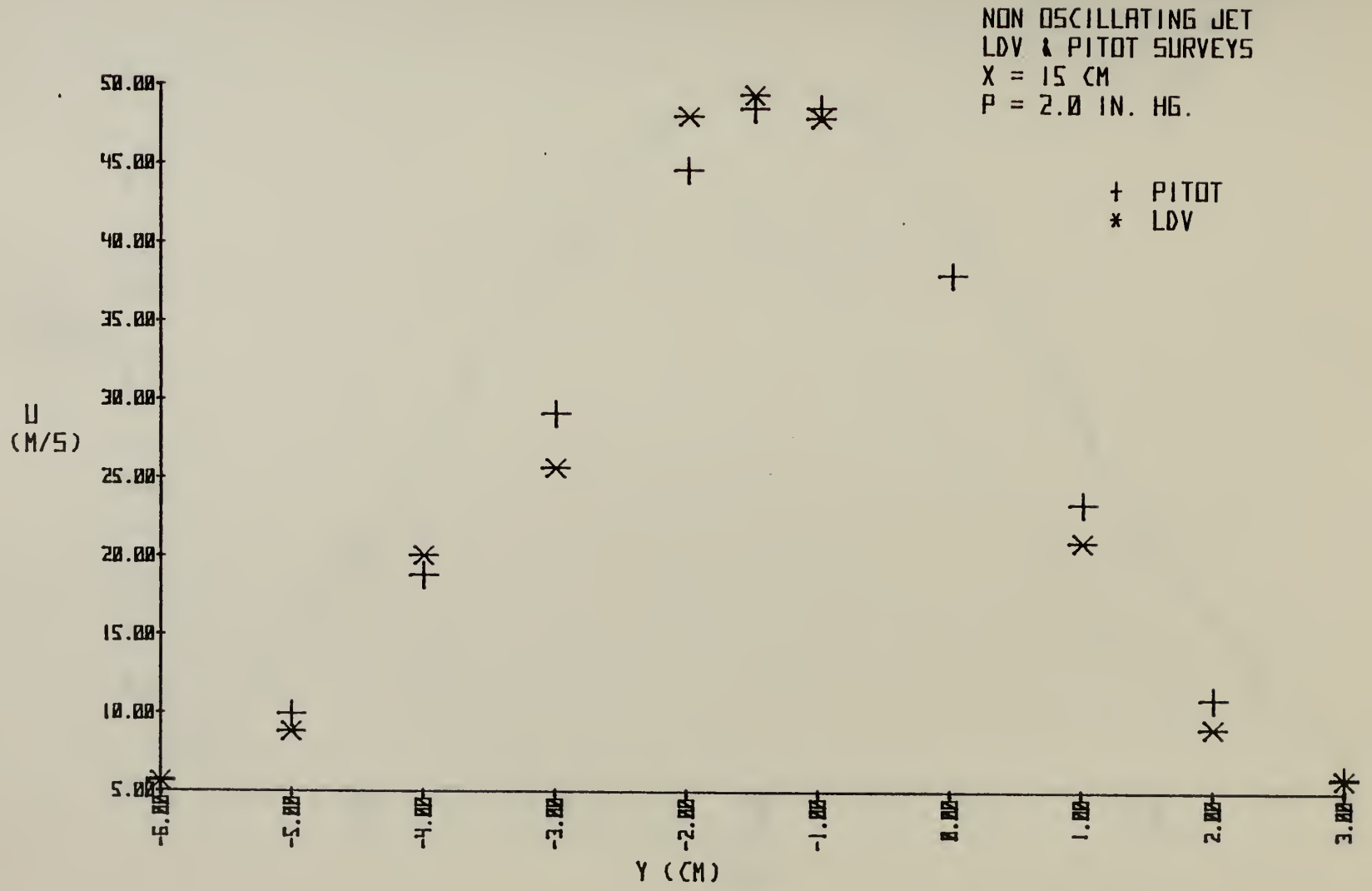
NON OSCILLATING JET
LDV & PITOT SURVEYS
X = 15 CM
P = 2.0 IN. HG.
+ PITOT
* LDV
U
(M/S)
50.00
45.00
40.00
35.00
30.00
25.00
20.00
15.00
10.00
5.00
-6.00
-5.00
-4.00
-3.00
-2.00
-1.00
0.00
1.00
2.00
3.00
Y ((CM)

FIGURE 21

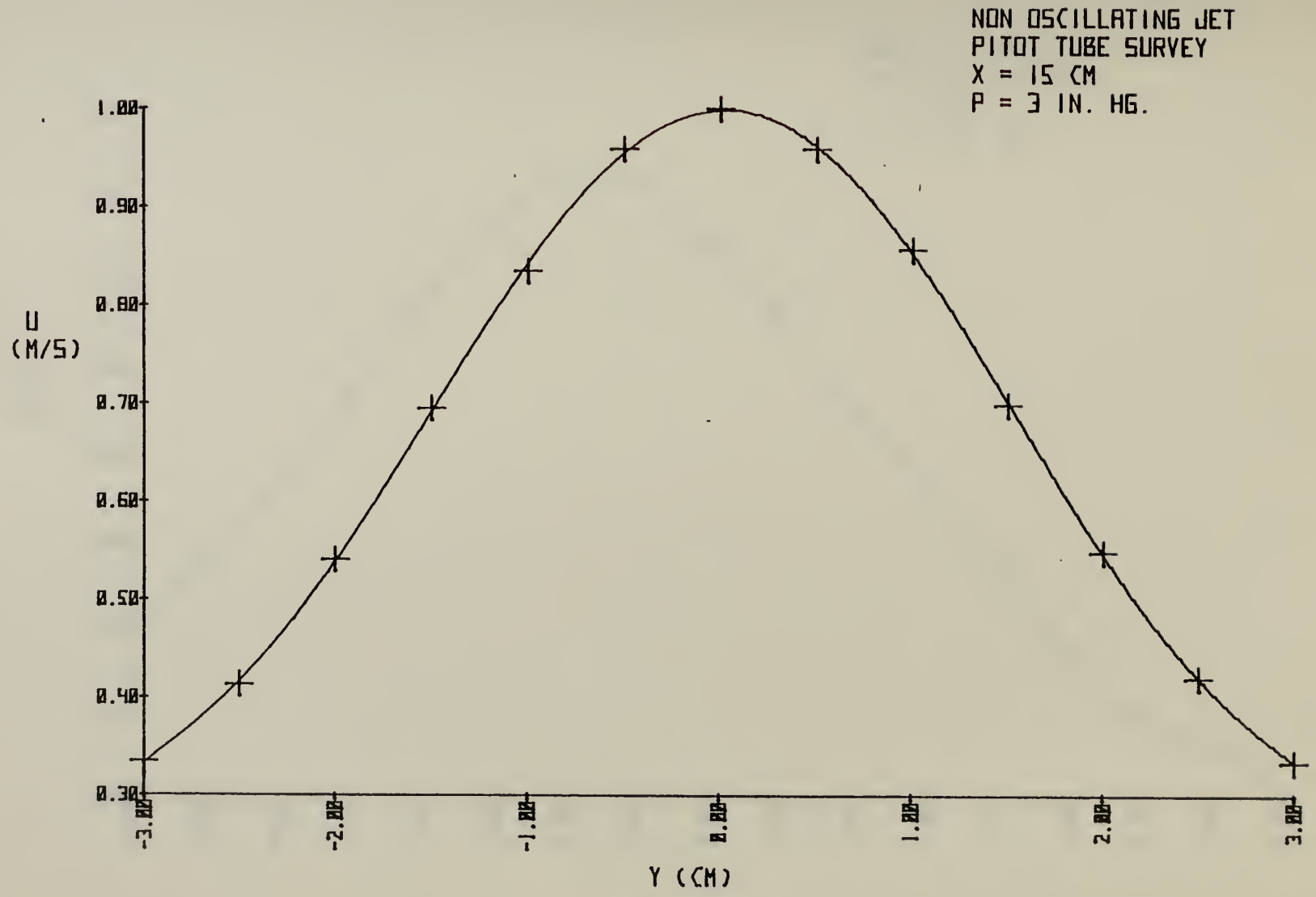
NON OSCILLATING JET
PITOT TUBE SURVEY
X = 15 CM
P = 3 IN. HG.
U
(M/S)
1.00
0.90
0.80
0.70
0.60
0.50
0.40
0.30
-3.00
-2.00
-1.00
0.00
1.00
2.00
3.00
Y (CM)

FIGURE 22

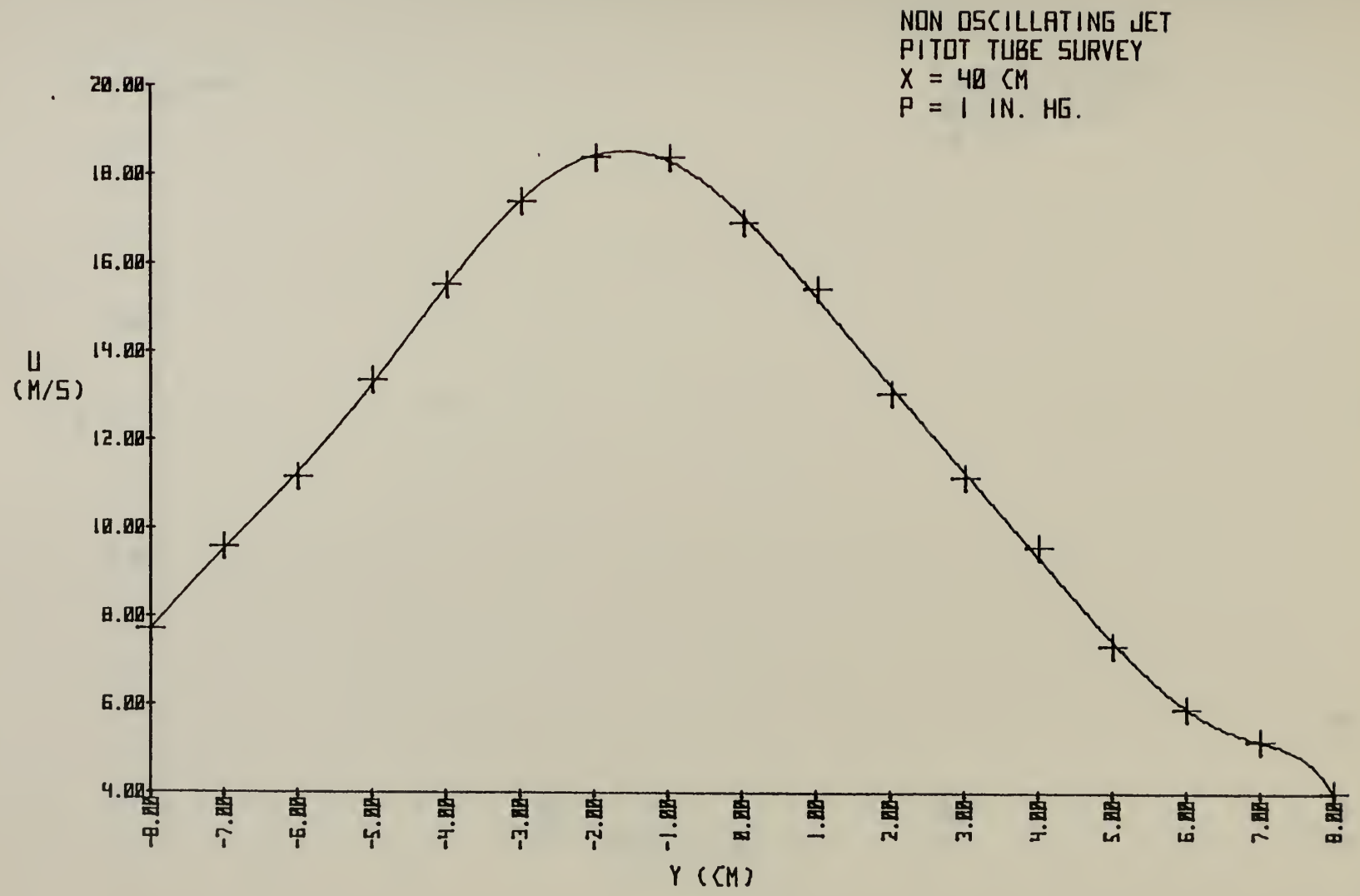
NON OSCILLATING JET
PITOT TUBE SURVEY
X = 40 CM
P = 1 IN. HG.
U
(M/S)
20.00
18.00
16.00
14.00
12.00
10.00
8.00
6.00
4.00
-8.00
-7.00
-6.00
-5.00
-4.00
-3.00
-2.00
-1.00
0.00
1.00
2.00
3.00
4.00
5.00
6.00
7.00
8.00
Y (CM)

FIGURE 23

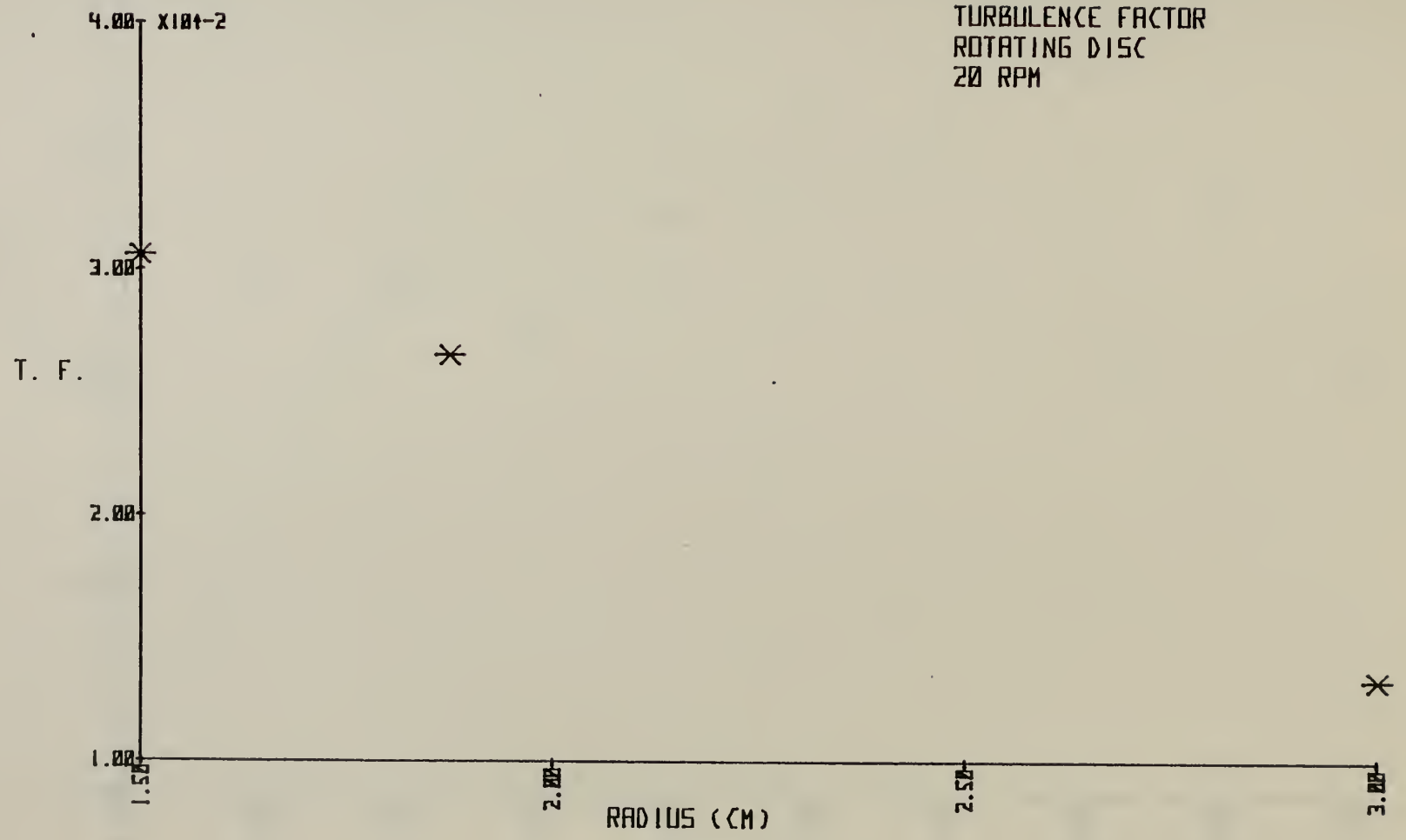
TURBULENCE FACTOR
ROTATING DISC
20 RPM
4.00 X10+-2
3.00
2.00
1.00
T. F.
1.50
2.00
2.50
3.00
RADIUS (CM)

FIGURE 24

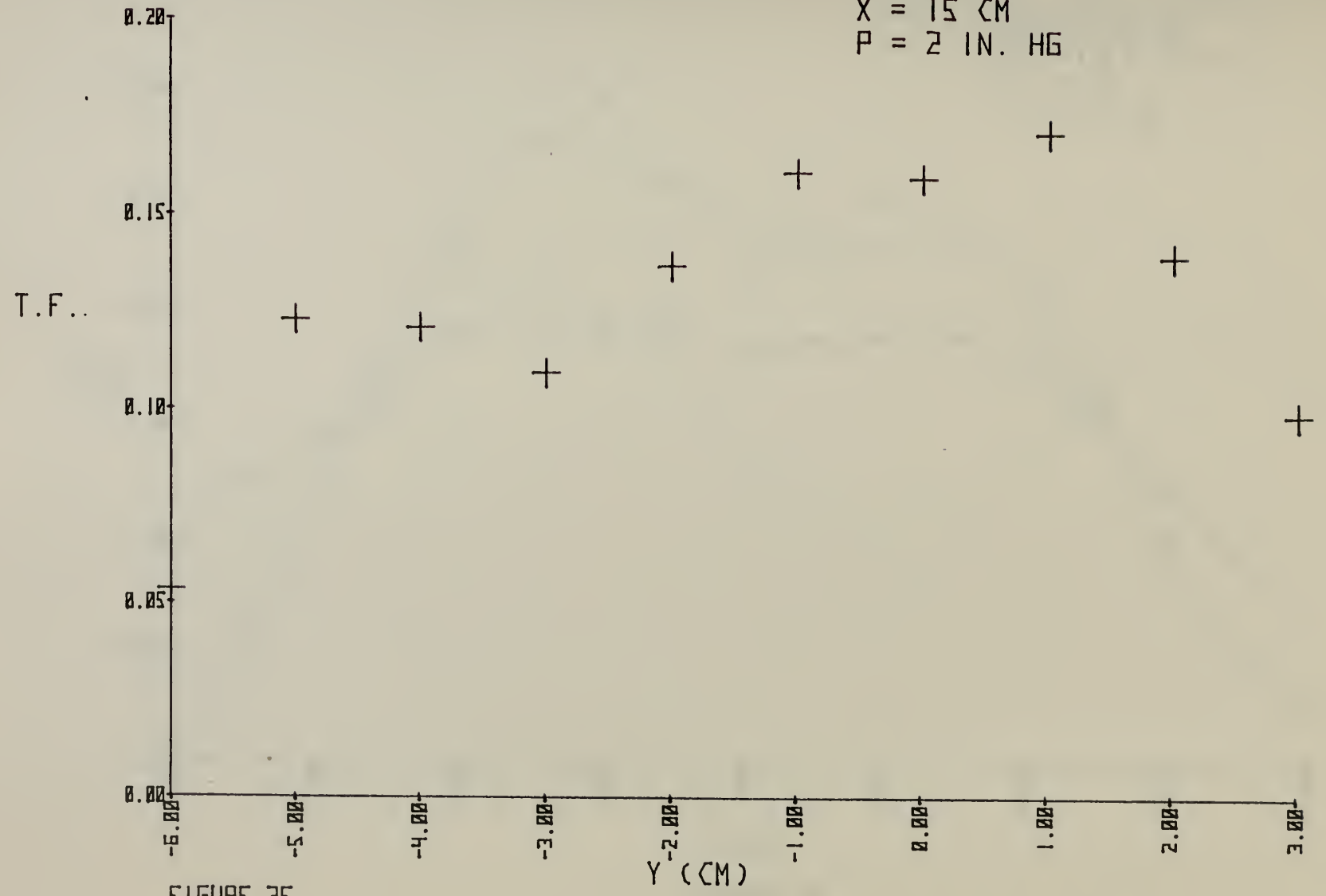
TURBULENCE FACTOR SURVEY
X = 15 CM
P = 2 IN. HG
T.F..
0.20
0.15
0.10
0.05
0.00
-6.00
-5.00
-4.00
-3.00
-2.00
-1.00
0.00
1.00
2.00
3.00
Y ((CM)

FIGURE 25

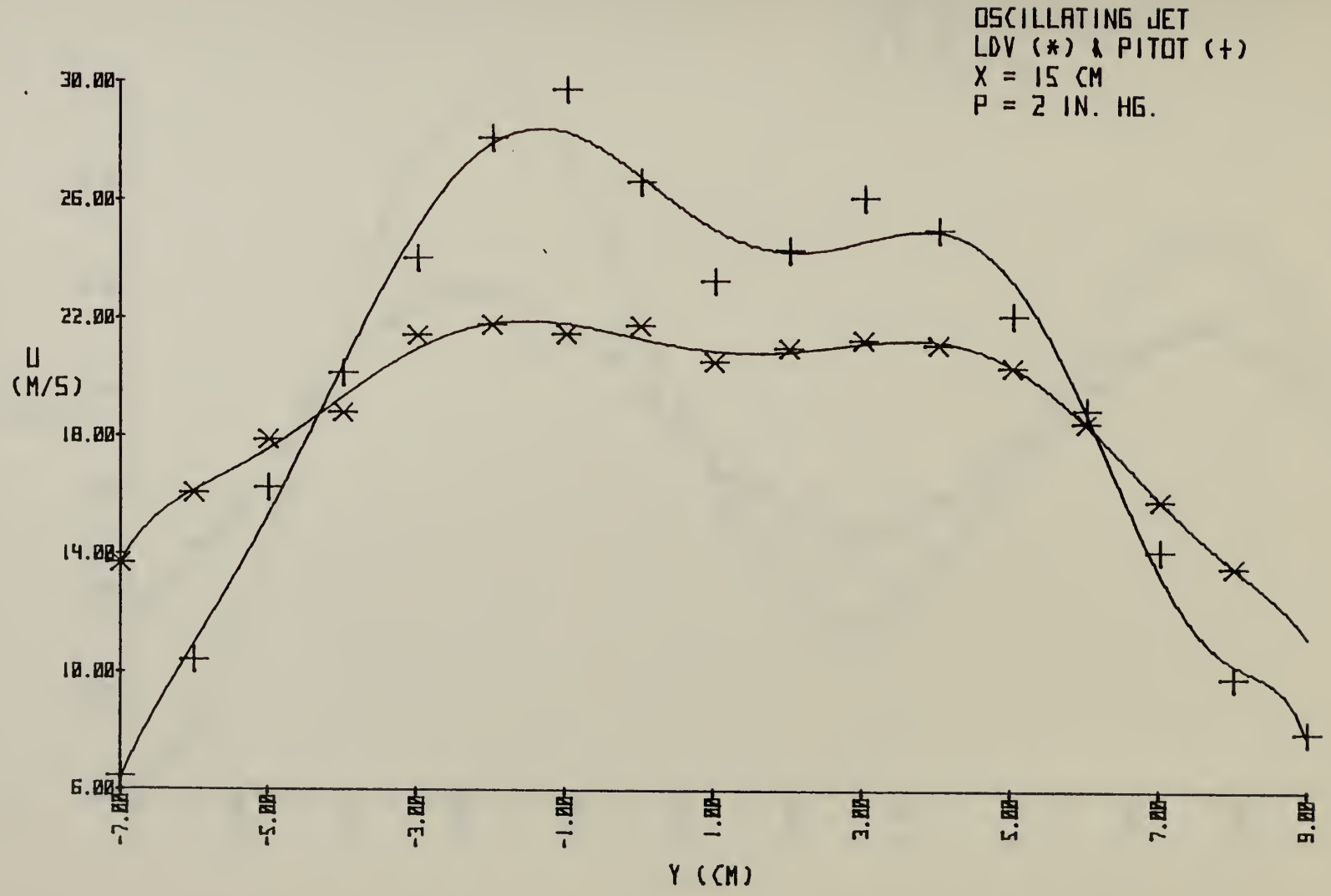
OSCILLATING JET
LDV (*) & PITOT (+)
X = 15 CM
P = 2 IN. HG.
30.00
26.00
22.00
18.00
14.00
10.00
6.00
U
(M/S)
-7.00
-5.00
-3.00
-1.00
1.00
3.00
5.00
7.00
9.00
Y (CM)

FIGURE 26

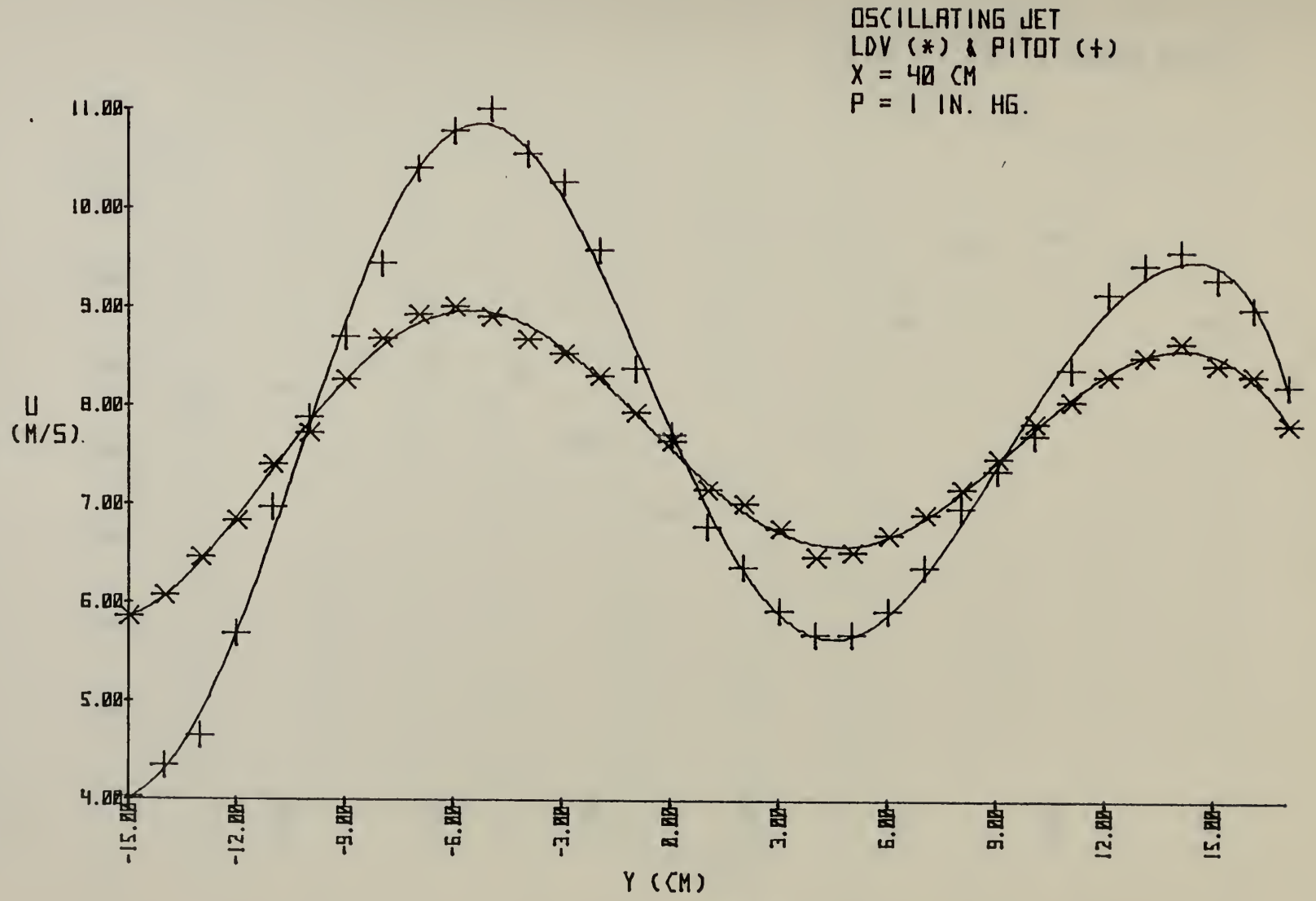
OSCILLATING JET
LDV (*) & PITOT (+)
X = 40 CM
P = 1 IN. HG.
U (M/S)
11.00
10.00
9.00
8.00
7.00
6.00
5.00
4.00
-15.00
-12.00
-9.00
-6.00
-3.00
0.00
3.00
6.00
9.00
12.00
15.00
Y (CM)

FIGURE 27

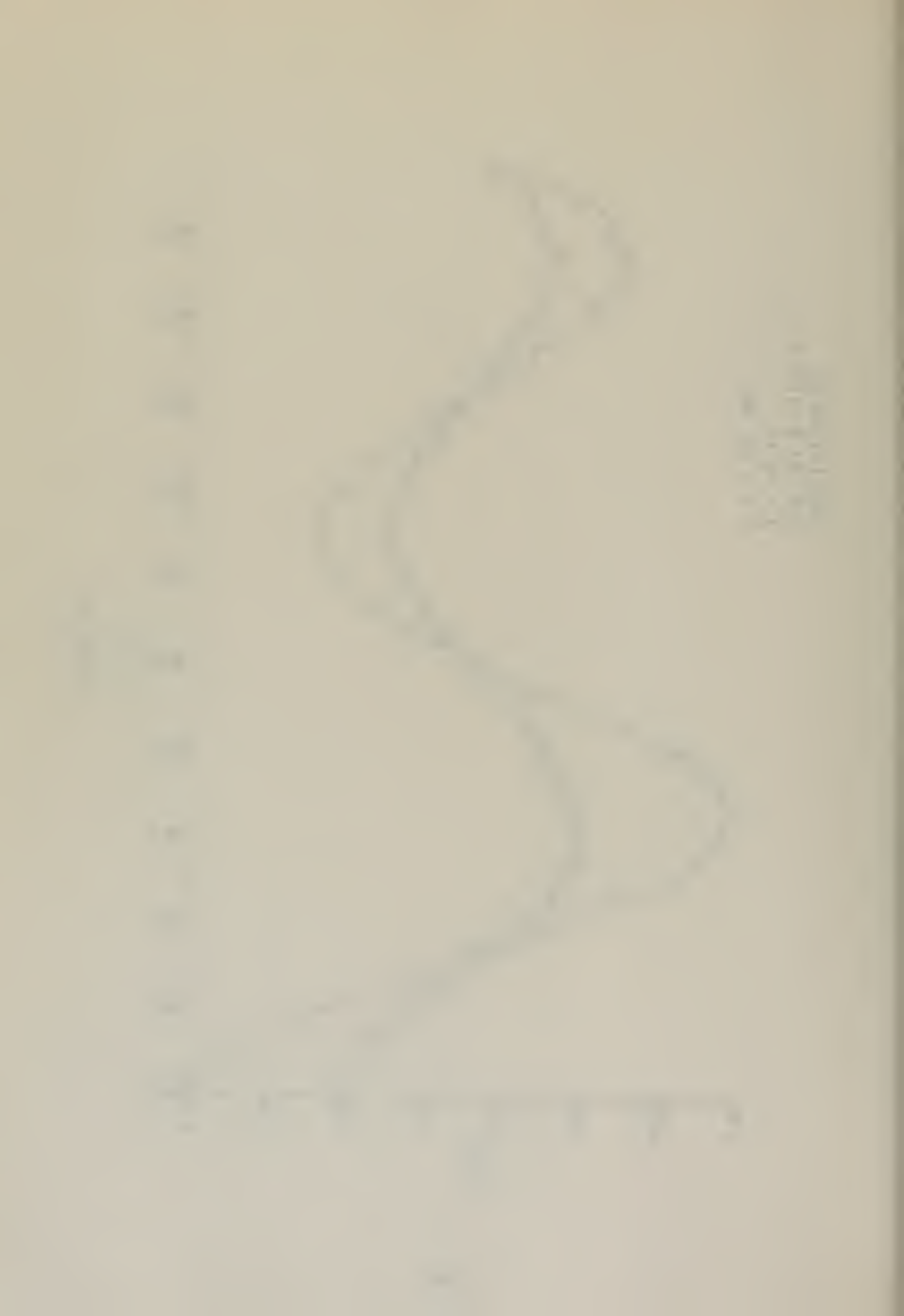

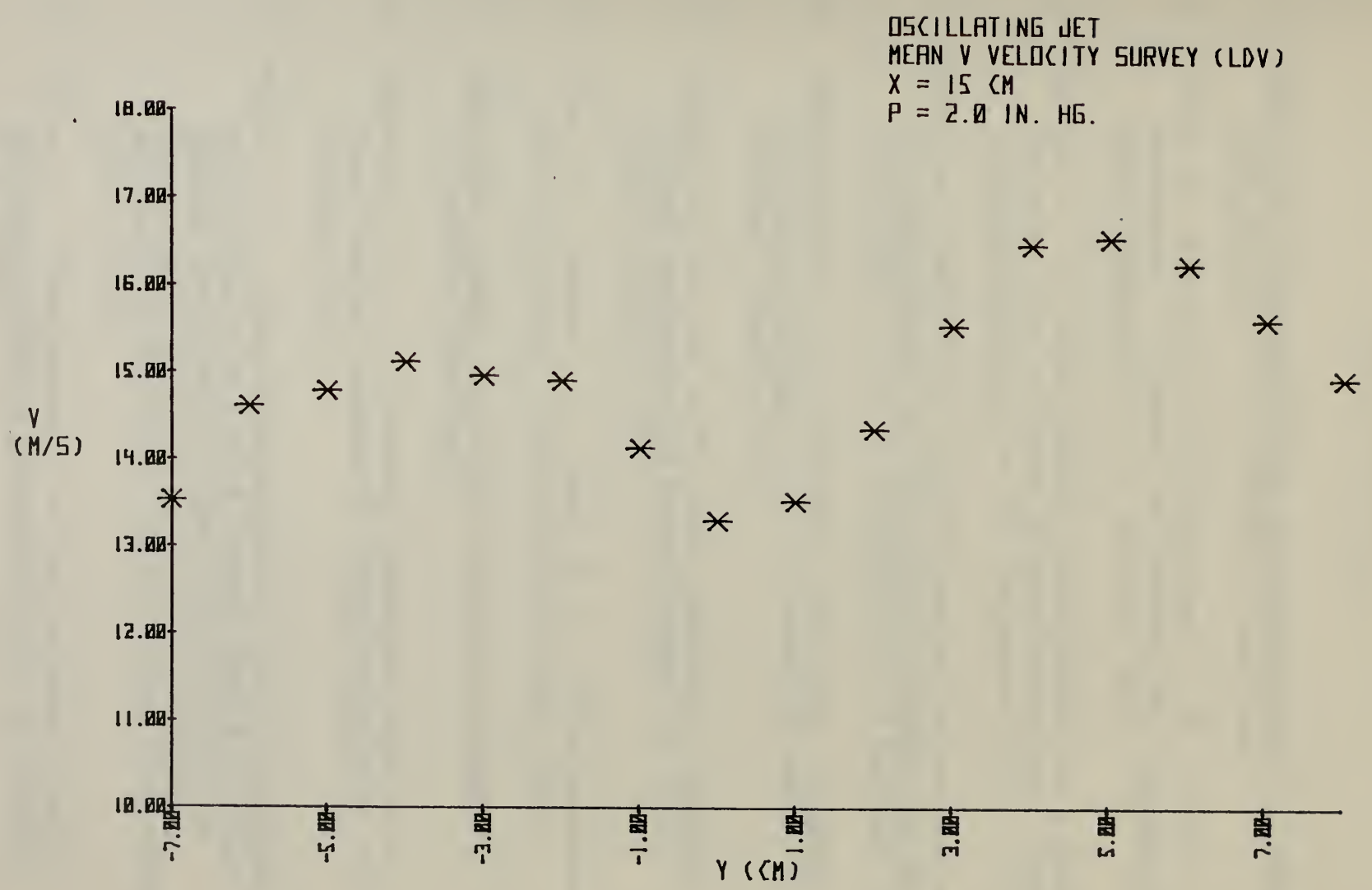
OSCILLATING JET
MEAN V VELOCITY SURVEY (LDV)
X = 15 CM
P = 2.0 IN. HG.
V
(M/S)
18.00
17.00
16.00
15.00
14.00
13.00
12.00
11.00
10.00
-7.00
-5.00
-3.00
-1.00
1.00
3.00
5.00
7.00
Y (CM)

FIGURE 28

LIST OF REFERENCES

1. DISA Type 556 Laser Doppler Anemometer Mark II Instruction Manual, DISA Information Department.

2. Durst, F., Melling A., and Whitelaw, J. H., "Laser Anemometry: A Report on Euromech 36," Journal of Fluid Mechanics, v. 56, November 1972.

3. Barker, S. J., "Laser-Doppler Measurements on a Round Turbulent Jet in Dilute Polymer Solutions," Journal of Fluid Mechanics, v. 60, September 1973.

4. vonKarman Institute for Fluid Dynamics Lecture Series 54, Measurements of Velocities in Single and Two-Phase Flows, by M. L. Riethmuller, 19 February 1973.

5. AGARDograph No. 215 on Fluidics Technology, Fluidic Sensors - A Survey, by A. E. Schmidlin and J. M. Kirshner, January 1976.

6. ABARDograph No. 215 on Fluidics Technology, Digital Fluidic Component and System Design, by G. A. Parker, January 1976.

7. Viets, H., Balster, D., Tomms, H. L., "Time Dependent Fuel Injectors," Wright Patterson AFB, Ohio.

8. DISA 55L90 Counter Processor Instruction Manual, DISA Information Department.

9. Steenstrup, F. V., "Counting Techniques Applied to Laser Doppler Anemometry," DISA Information, No. 18, September 1975.

10. Malik, I. A., Flow Visualization of the Turbulent Jet at the Exit of a Single Element Nozzle by Holographic Technique, and Mean Velocity Profile Measurements with a Laser Doppler Anemometer, Aeronautical Engineer's Thesis, Naval Postgraduate School, 1976.

11. Viets, H., "Development of a Time Dependent Nozzle," Aerospace Research Laboratories AFL TR 74-0113, August 1974.

INITIAL DISTRIBUTION LIST

		No. Copies
1.	Defense Documentation Center Cameron Station Alexandria, Virginia 22314	2
2.	Library, Code 0212 Naval Postgraduate School Monterey, California 93940	2
3.	Department Chairman, Code 67 Department of Aeronautics Naval Postgraduate School Monterey, California 93940	1
4.	Professor D. J. Collins, Code 67Co Department of Aeronautics Naval Postgraduate School Monterey, California 93940	1
5.	Professor Max F. Platzer Department of Aeronautics Naval Postgraduate School Monterey, California 93940	1
6.	LT Michael K. Hollis 139 Dunecrest Avenue Monterey, California 93940	1

25 JAN 77
19 JAN 78
6 FEB 78
1 JUN 78
30 JAN 80
24246
24960
24960
24960
26166

Thesis
H6858 Hollis
c.1
166682
Measurement of instantaneous velocities from a fluidically controlled nozzle using a laser Doppler velocimeter.
25 JAN 77
1 JUN 78
30 JAN 80
24246
26166

Thesis
H6858 Hollis
c.1
166682
Measurement of instantaneous velocities from a fluidically controlled nozzle using a laser Doppler velocimeter.

thesH6858
Measurement of instantaneous velocities
3 2768 002 06915 5
DUDLEY KNOX LIBRARY